TropWATER
Centre for Tropical Water and Aquatic Ecosystem Research

JCU

Monitoring mangrove threats across the Torres Straits using remote-sensing

May 2022 | Report No. 22/23

Authored by: Adam Canning & Norm Duke

Monitoring mangrove threats across the Torres Straits using remote-sensing

Centre for Tropical Water & Aquatic Ecosystem Research (TropWATER) James Cook University

Townsville Phone : (07) 4781 4262 Email:

TropWATER@jcu.edu.au

Web: www.jcu.edu.au/tropwater/

The report may be cited as

Canning, A & Duke, N (2022). *Monitoring mangrove threats across the Torres Straits using remote-sensing (Report No. 22/23)*. Centre for Tropical Water and Aquatic Ecosystem Research, James Cook University.

Contacts

For more information contact: Adam Canning, adam.canning@jcu.edu.au, 07 478 14292

Cover image: Supplied by Norm Duke and taken at Badu Island in Torres Strait. Duplicated from:

Duke, N. C. (2014). Mangrove Coast. In *Encyclopedia of Earth Sciences Series: Vol. Part 2* (pp. 1–17). Springer, Dordrecht. https://doi.org/10.1007/978-94-007-6644-0_186-1

Contents

Introduction

Mangroves are most prevalent forested ecosystem in the Torres Strait, providing immense cultural, ecological and economic value. The benefits to humans arising from mangroves (and nature in general) are known as 'ecosystem services'. Those most relevant to Torres Strait Islanders include the provision of fish and prawn habitat and fisheries; shoreline protection; carbon sequestration and storage, buffering against climate change; the improvement of water quality from catchment runoff; provision of habitat for biodiversity; and cultural heritage and traditional use values. With this study, we utilise another key benefit where mangroves are valuable indicators of change, and the drivers of change (Duke et al., 2021).

As sea levels rise and shorelines become eroded, healthy mangrove forests will become increasingly essential to the protection of land-based activities from tidal inundation and storm storge. Reduced habitat condition, reduced biodiversity and habitat complexity and altered ecosystem processes reduce the capacity of mangroves to withstand climate impacts and their capacity of mangroves to buffer these impacts and protect adjacent coastal areas (Gilman et al., 2008; Chow, 2017; Ward et al., 2017).

Despite their importance, mangroves continue to be directly destroyed and degraded by poor catchment and coastal zone management. Approximately 62% of the global mangrove loss occurring between 2000 and 2016 resulted from land use change to aquaculture and agriculture (Goldberg et al., 2020). Despite legal protections in Queensland, mangroves continue to be destroyed or threatened by activities, such as altered hydrology, harvesting, development, pollution, and climate change.

While climate change cannot be prevented at the local scale, reducing local stressors can help improve the resilience of mangroves to withstand the impacts of climate change, and continue to deliver ecosystem services, such as coastline protection (Gilman et al., 2008; Chow, 2017; Ward et al., 2017). By understanding the long-term impacts of climate change and localised stressors, then local actions can be adapted to better reduce the localised stress mangroves face and ensure sustainable use. This was further echoed in the latest Torres Strait State of Environment reporting, indicating a reduction in outlook for mangroves from 'good' in 2016 to having 'significant concern' in 2021 (TSRA, 2021). The report also identified the need for greater support for rangers to build capacity in assessing and managing mangroves.

This report aims to demonstrate how remote sensing can be used to inform the long-term condition of mangrove forests in response to a range of threats or drivers of change across the Torres Straits. Given insights from previous examinations (Duke et al., 2015; 2021), the key drivers of change we focus on include: root burial, lightning gaps, depositional gain, ecotone shifts, cyclone damage, shoreline retreat and upland expansion, sea level oscillations, changing climatic conditions, mangrove clearing and harvesting, and fire damage. We then present our recommendations for developing a future mangrove monitoring program that seeks to utilise remote sensing across the Torres Straits.

Climatic & sea level conditions

The Australian Bureau of Meteorology was the primary source of climatic data (sea level, rainfall, and temperature); while Geoscience Australia was the primary source of long-term shoreline change.

Booby Island has the longest tide gauge record (station ID: 1268) in the Torres Straits. There are three other sites nearby in southern Torres Straits that show similar patterning, but there are no tide gauge sites available for the central and northern Torres Straits. Figures 1 and 2 show the mean sea level and the six-month rolling sea level anomaly (also known as the 'Sea Level Stress Index' by Duke et al (2022)) at Booby Island. The difference in data before and after the data gap during the 1980s should be viewed cautiously as this may represent a slight shift in position between old and new gauging equipment.

Long-term rainfall and temperature data were best available for Coconut Island and Horn Island (Figures 3-6).

Geoscience Australia's long-term (1988-2019) estimate of shoreline retreat or accretion was estimated by Landsat satellite estimated mean sea level, as described in Bishop-Taylor et al (2021a), and shown in Figures 7-10.

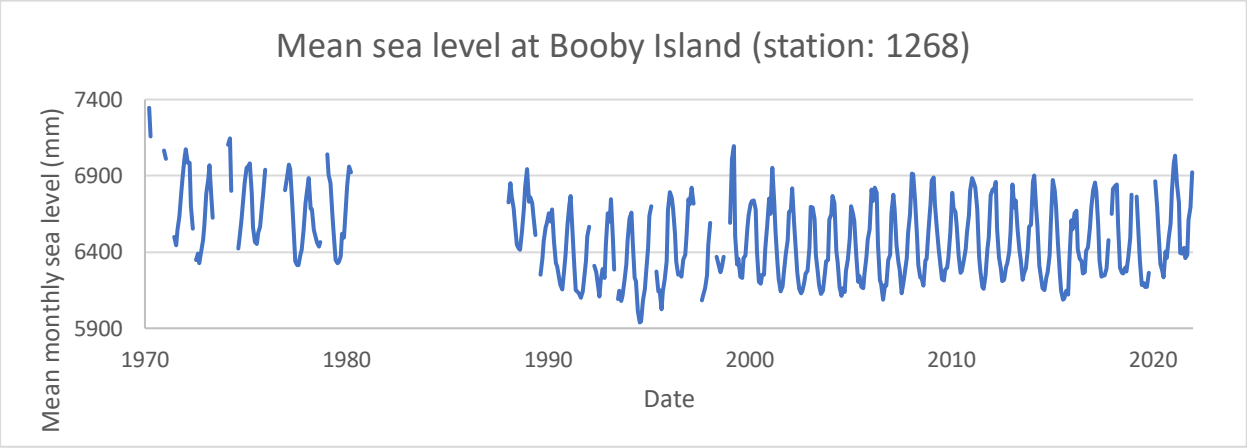

Figure 1. The mean sea level as measured at Booby Island tide gauge.

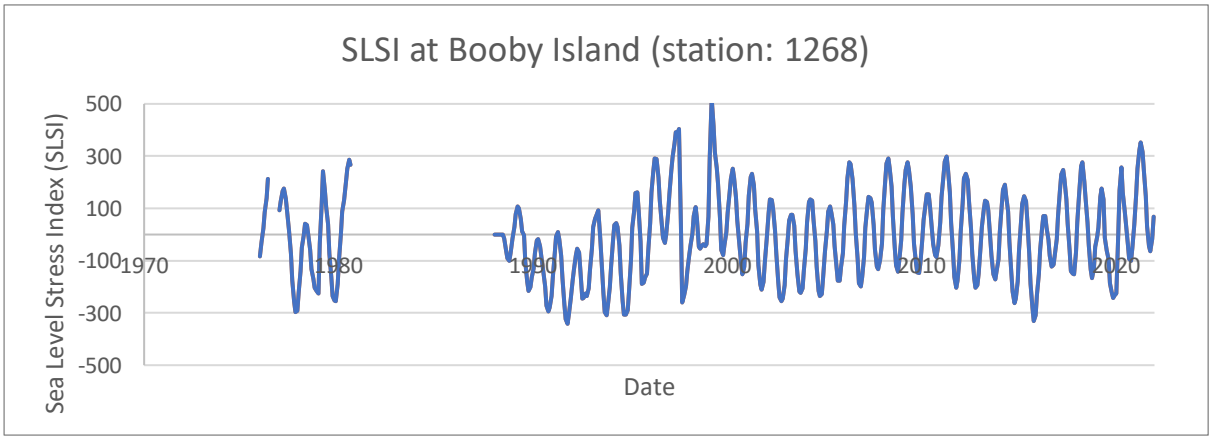

Figure 2. The six-month rolling anomaly of sea level (also known as the Sea Level Stress Index (SLSI; Duke et al (2022)) for the tide gauge at Booby Island.

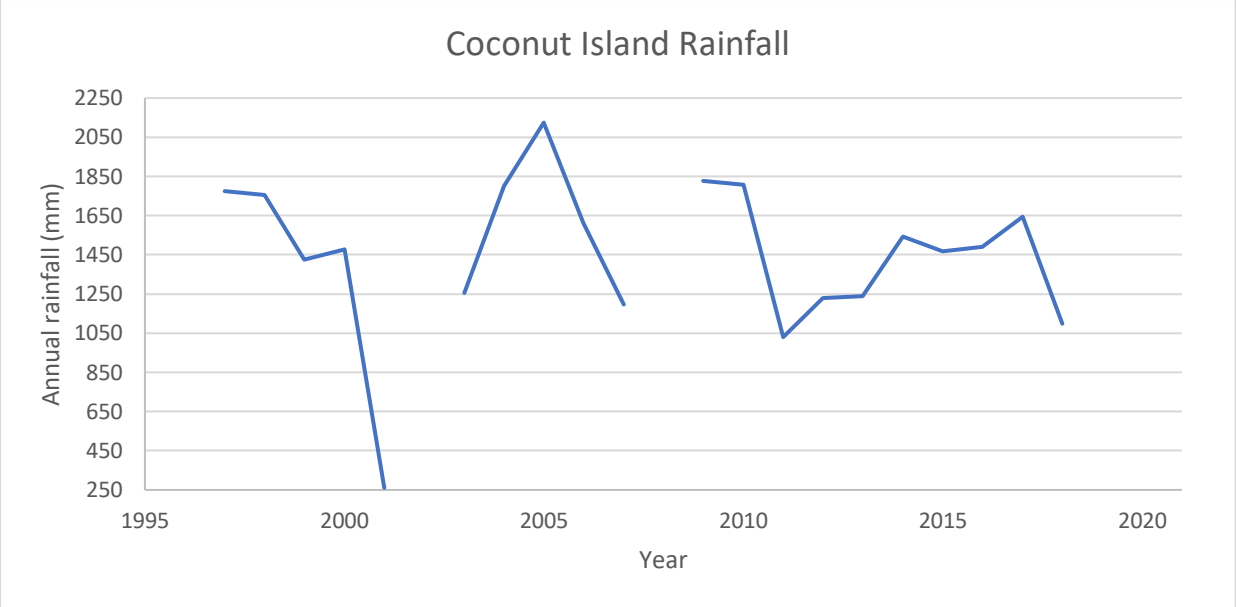

Figure 3. The total annual rainfall (mm) at Coconut Island.

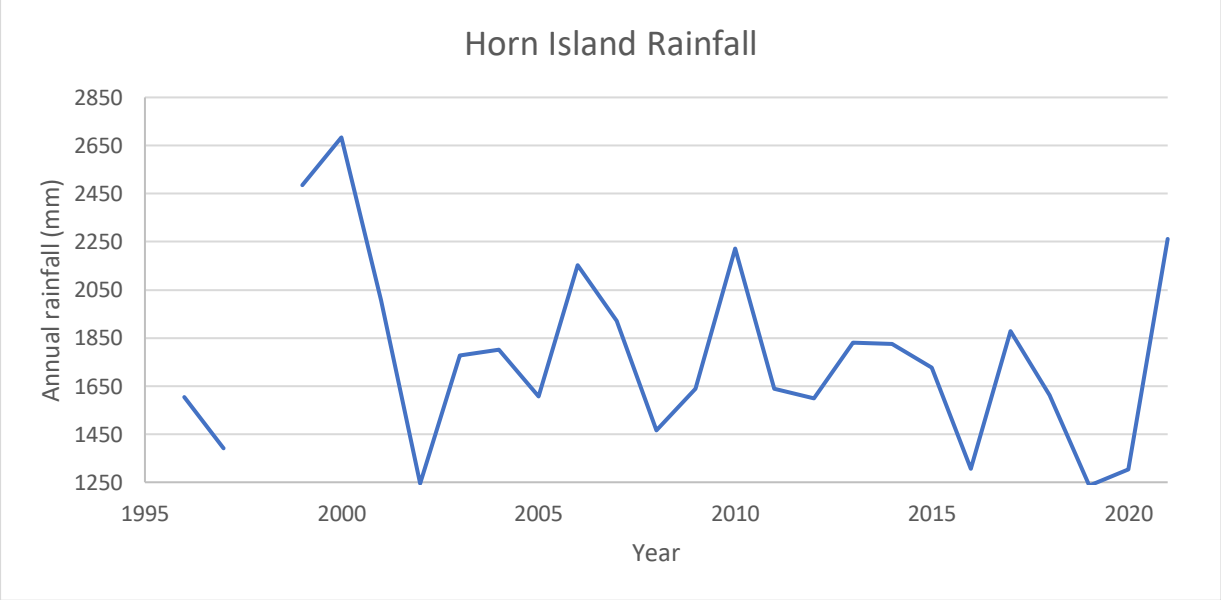

Figure 4. The total annual rainfall (mm) at Horn Island.

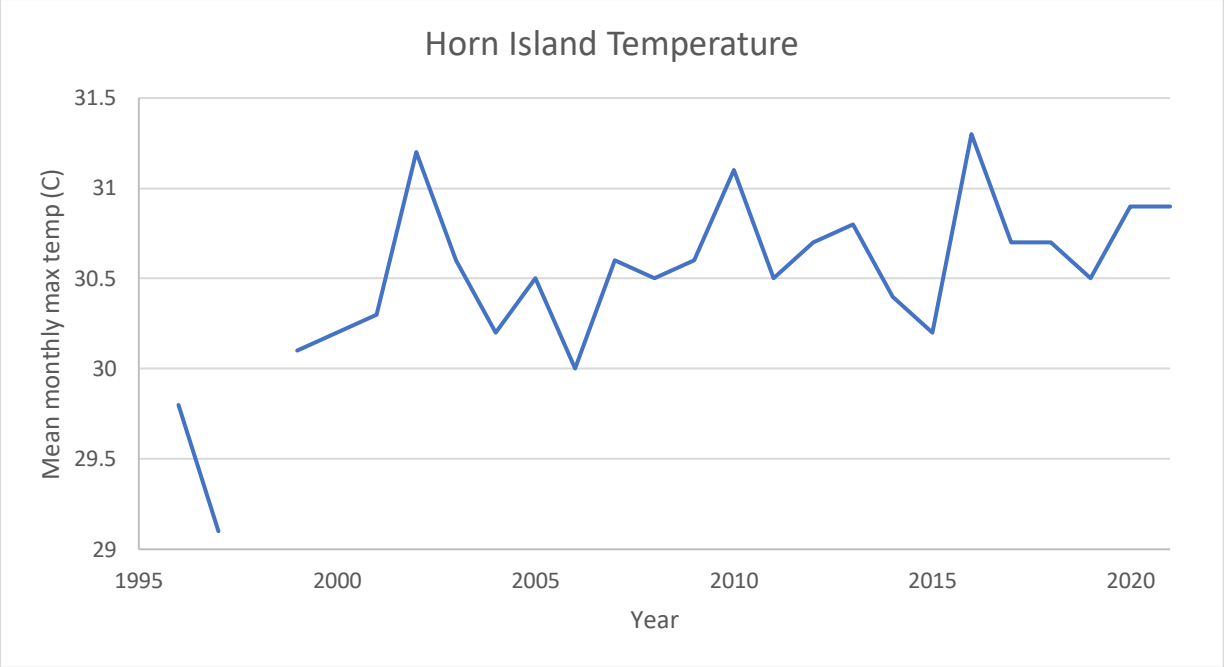

Figure 5. The mean monthly maximum daily temperature (degrees Celsius) at Horn Island.

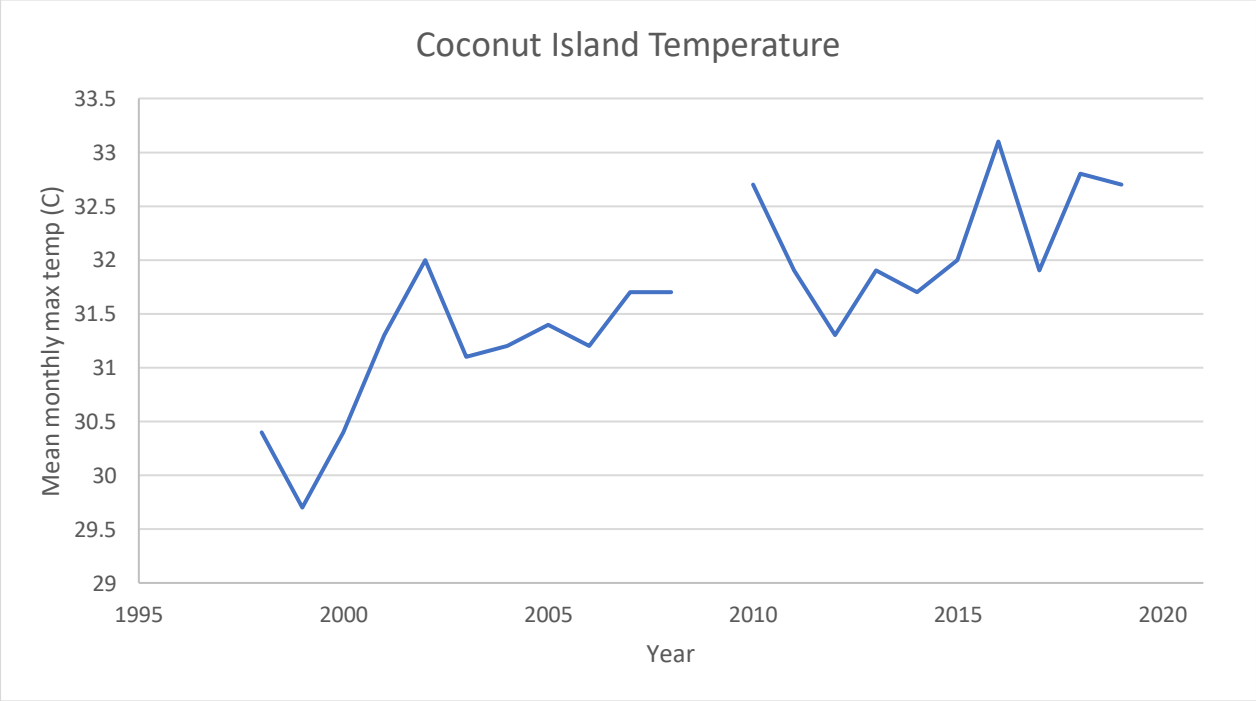

Figure 6. The mean monthly maximum daily temperature (degrees Celsius) at Coconut Island.

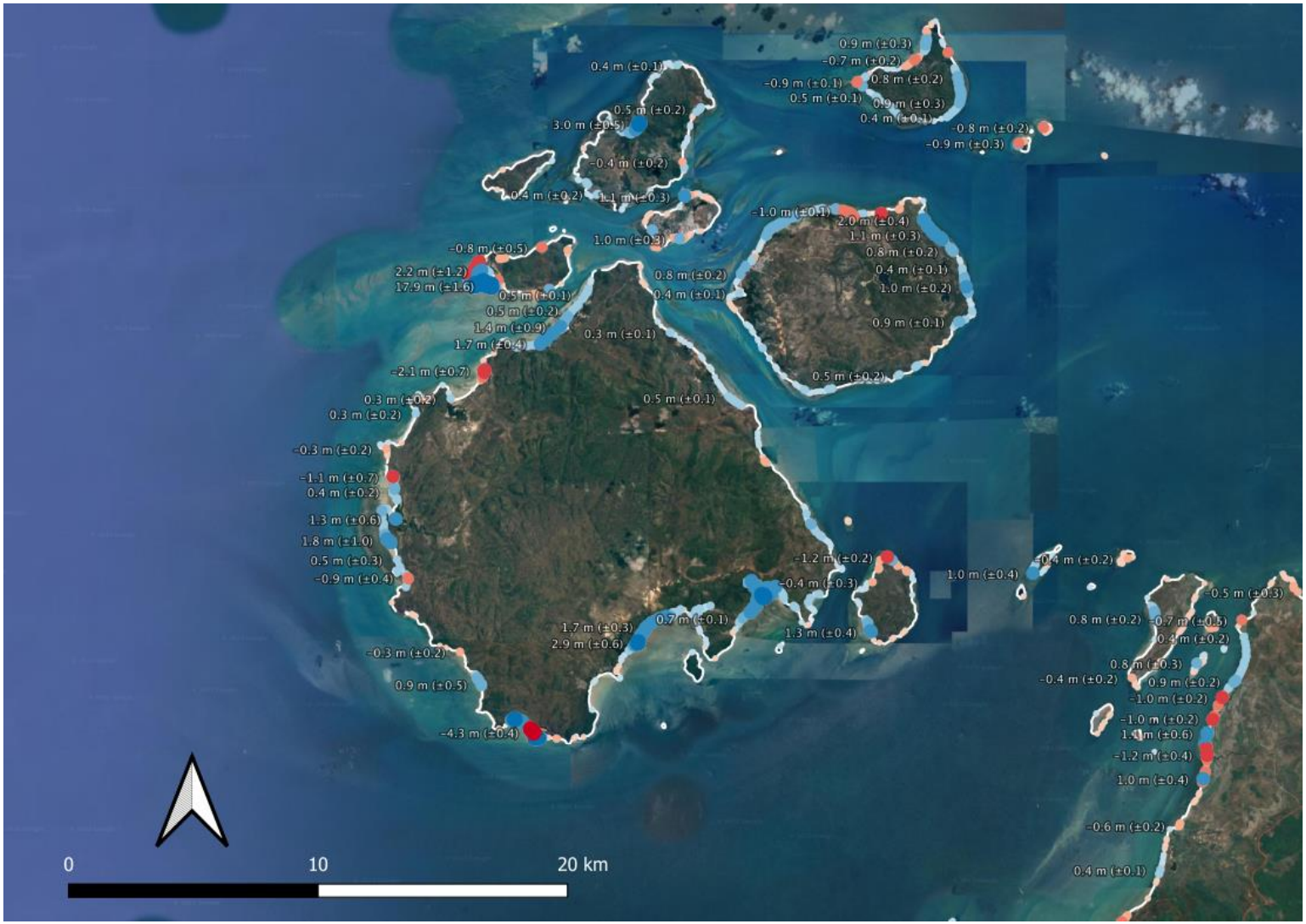

Figure 7. The long-term shoreline erosion (red) and accretion (blue), as predicted by Bishop-Taylor et al (2021a), between 1988-2019, at and around Prince of Wales and Thursday Islands.

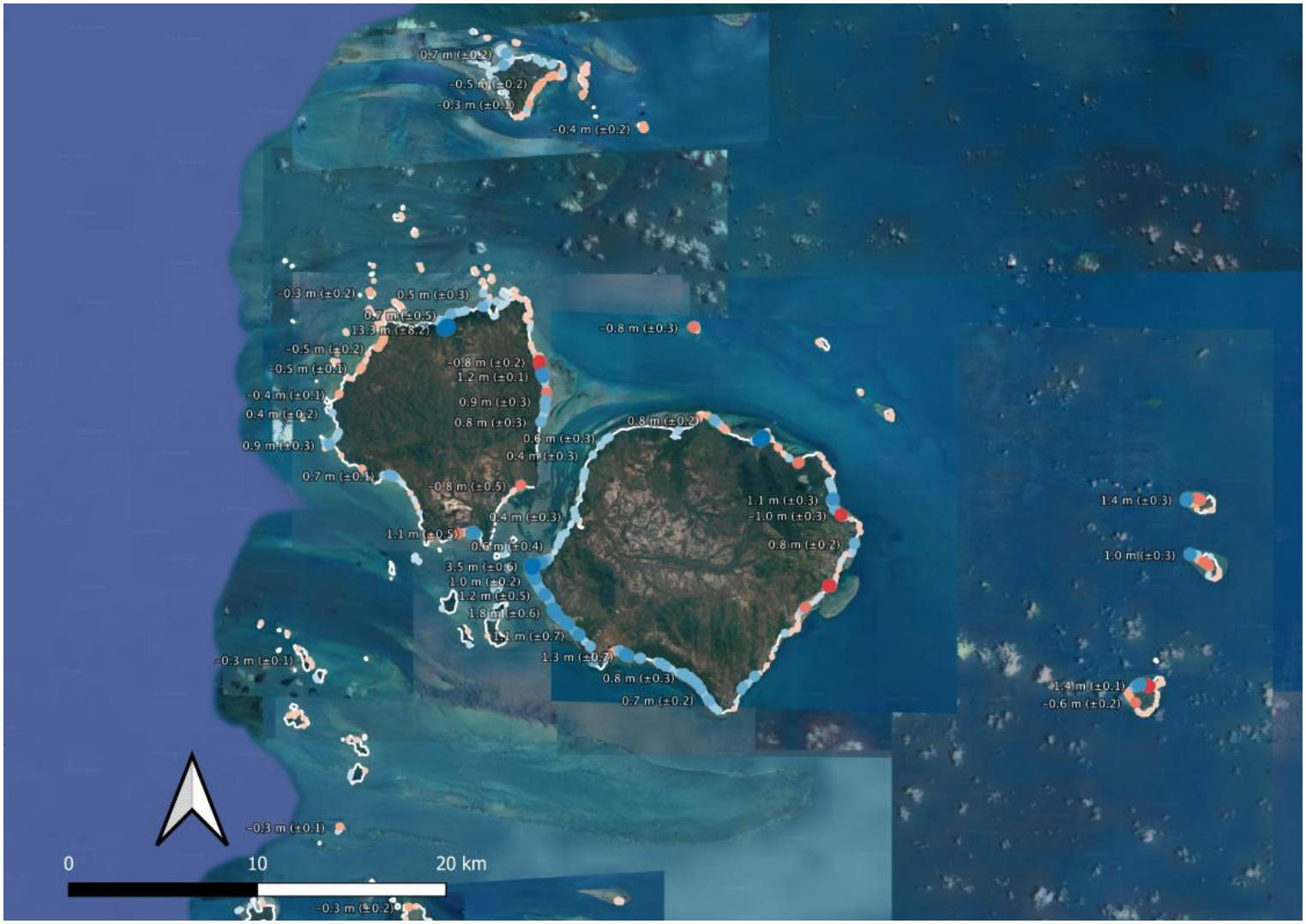

Figure 8. The long-term shoreline erosion (red) and accretion (blue), as predicted by Bishop-Taylor et al (2021a), between 1988-2019, at and around Moa Island.

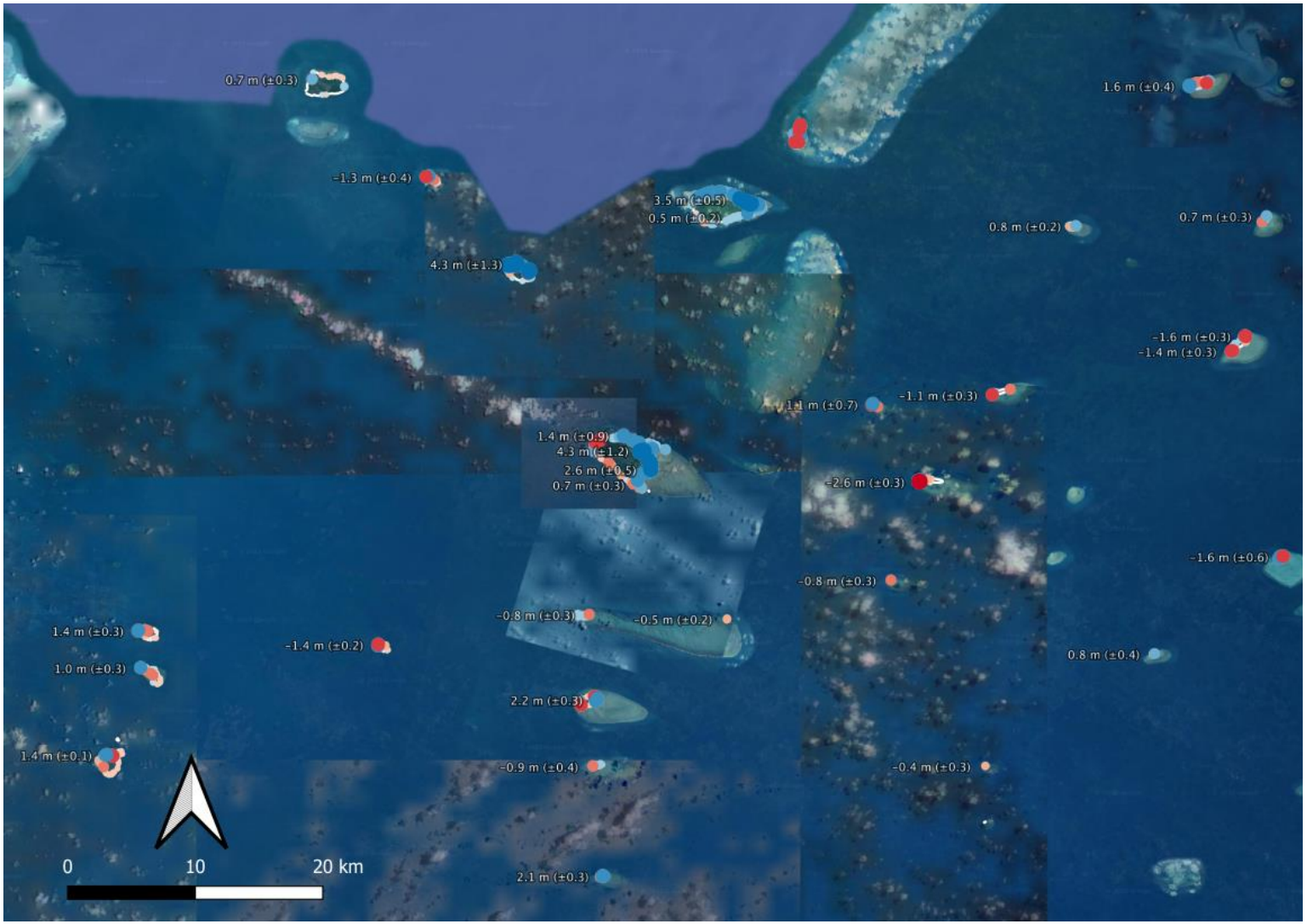

Figure 9. The long-term shoreline erosion (red) and accretion (blue), as predicted by Bishop-Taylor et al (2021a), between 1988-2019, at and around Iama Island.

Figure 10. The long-term shoreline erosion (red) and accretion (blue), as predicted by Bishop-Taylor et al (2021a), between 1988-2019, at and around Saibai Island.

Investigations into key drivers of change

To exemplify the applicability of satellite-based monitoring, we used long-term (1987-2021) Landsat imagery to calculate the NDVI (normalised difference vegetation index) as an indicator of mangrove canopy health at 217 locations across the entire extent of mangroves of the Torres Straits (Figures 13-19; Table A1). These locations were positioned at the front and back edges of the shoreline mangrove zone, and were identified using shoreline aerial surveys by Duke et al (2015), long-term (30 year) Landsat-informed changes in shoreline position by Bishop-Taylor et al (2021b), locations of previous mangrove surveys, and the authors' personal knowledge of mangrove stressors in the region. At each location, was also assigned a suspected driver of change (Table 1), and a change in the NDVI used as an indicator of whether the suspected change was realised in a change in canopy condition. At the outset, it is important to stress that while remote sensing may detect changes in canopy condition, that does not mean that other processes are not changing below the canopy.

The NDVI is a widely used metric to assess the 'greenness' of vegetation, including mangrove forests. Mathematically, the difference between near-infrared reflectance (which vegetation strongly reflects) and red light reflectance (which vegetation absorbs; Figure 11), and calculated as:

$$NDVI = (near\text{-}infrared - red)/(near\text{-}infrared + red)$$

Scores range between -1 and 1, with living plants between 0 and 1. The higher the value, the healthier the plant.

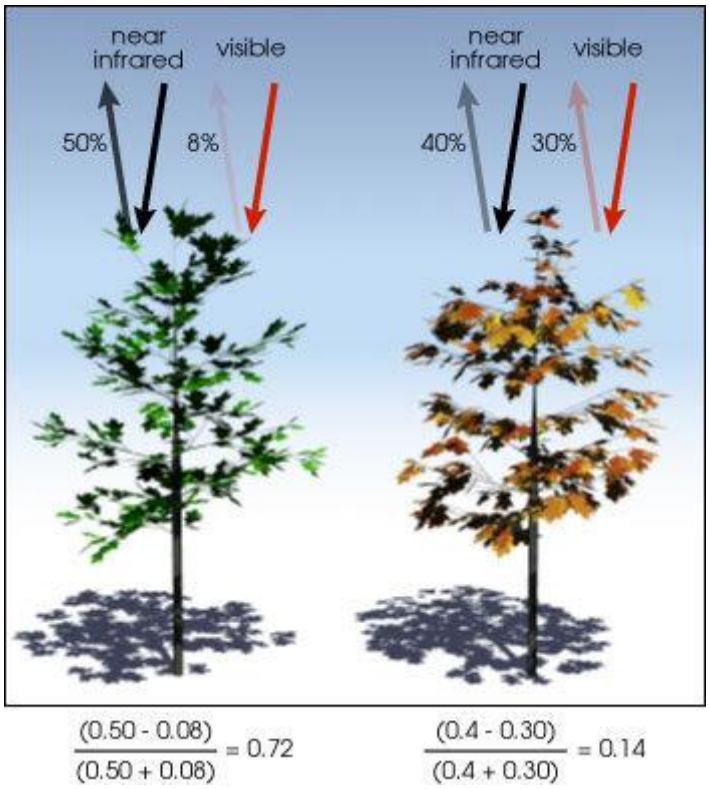

Figure 11. An example calculation of the NDVI for a healthy and an unhealthy plant. Sourced from:

https://earthobservatory.nasa.gov/features/MeasuringVegetation/measuring_vegetation_2.php

Figure 12. An approximate guide to interpreting NDVI scores. Sourced from:

https://eos.com/blog/ndvi-faq-all-you-need-to-know-about-ndvi/

Table 1. The nominal drivers of change and code assigned to each sample location across the Torres Straits.	
Code	Nominal driver
ROOT	Root Burial
LiG	Light Gap
D&D	Desiccation & Drowning Dieback
DeG	Depositional Gain
ES-ve	Ecotone Shift Negative
ES+ve	Ecotone Shift Positive
CyL	Cyclone
ReTr	Shoreline Retreat
EXP	Expansion upland
CUT	Cutting Harvest
POLN	Pollution
BURNT	Fire Damage
IFC	Inner Fringe Collapse
TAI	Desiccation Dieback
XM	Xylocarpus mollucensis phenology

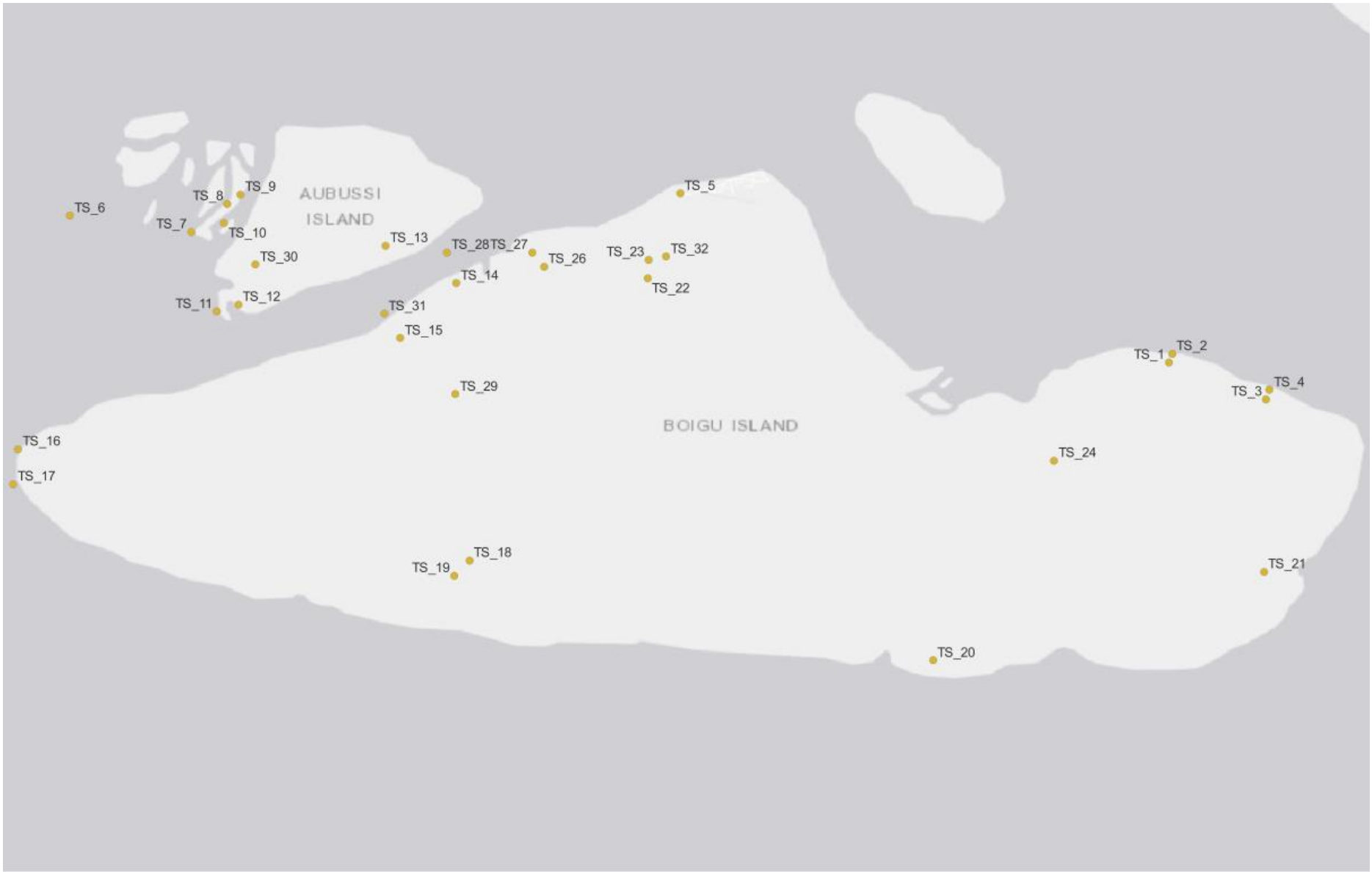

Figure 13. The long-term NDVI sample sites at and around Boigu Island, estimated from Landsat imagery between 1987 and 2021.

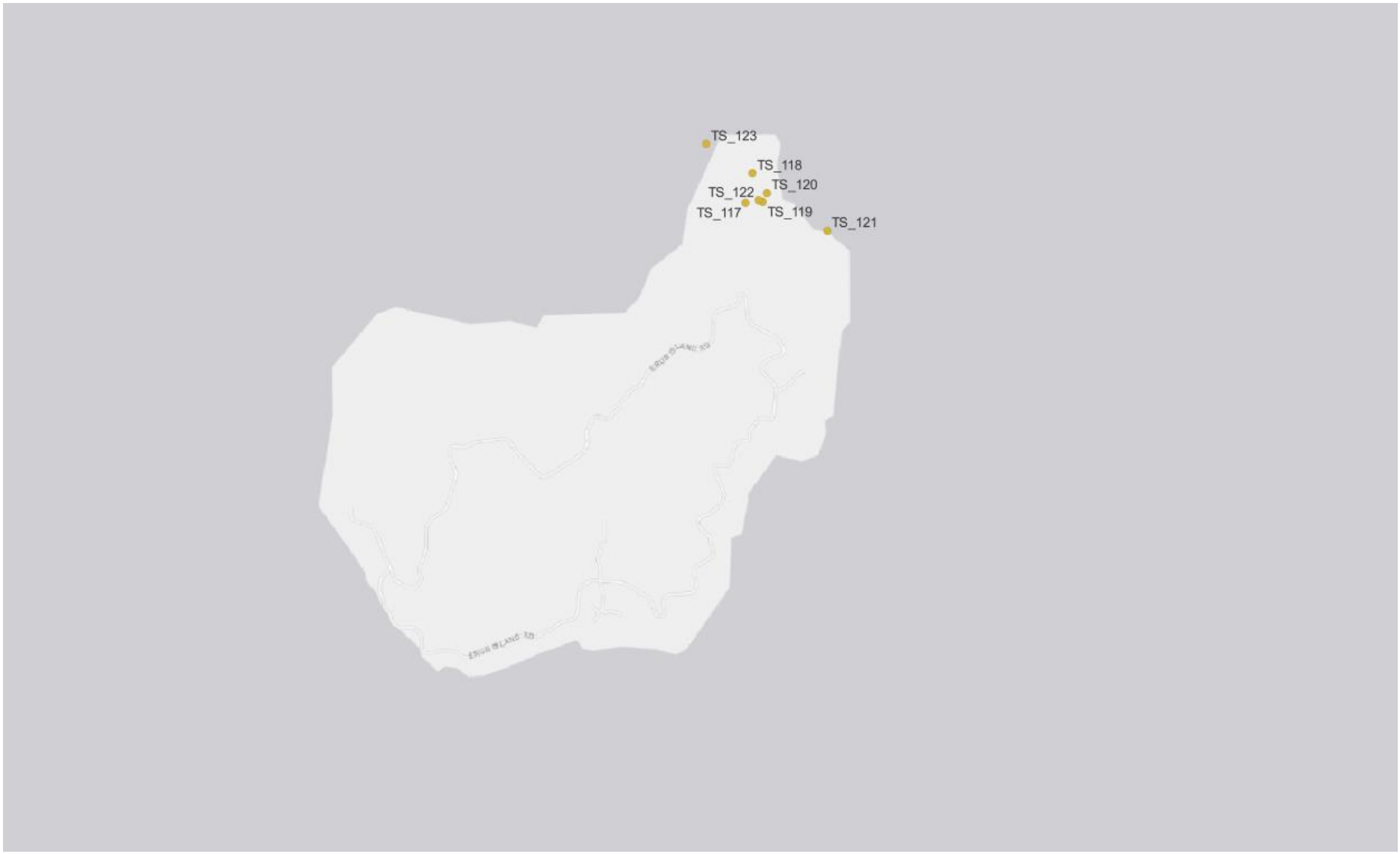

Figure 14. The long-term NDVI sample sites at Erub Island, estimated from Landsat imagery between 1987 and 2021.

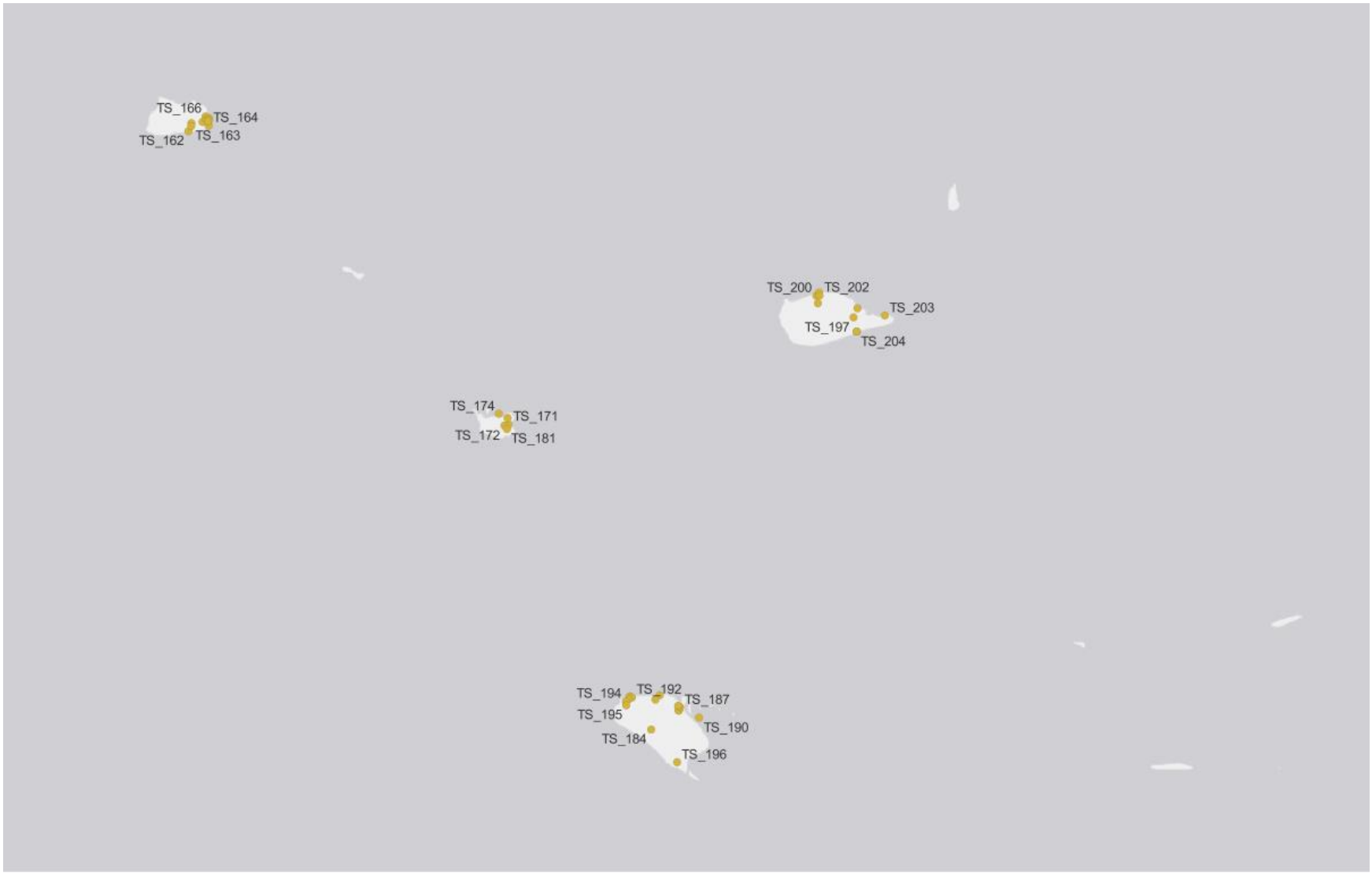

Figure 15. The long-term NDVI sample sites at and around the central islands (Gabba, Iama, Sassie, Zagai), estimated from Landsat imagery between 1987 and 2021.

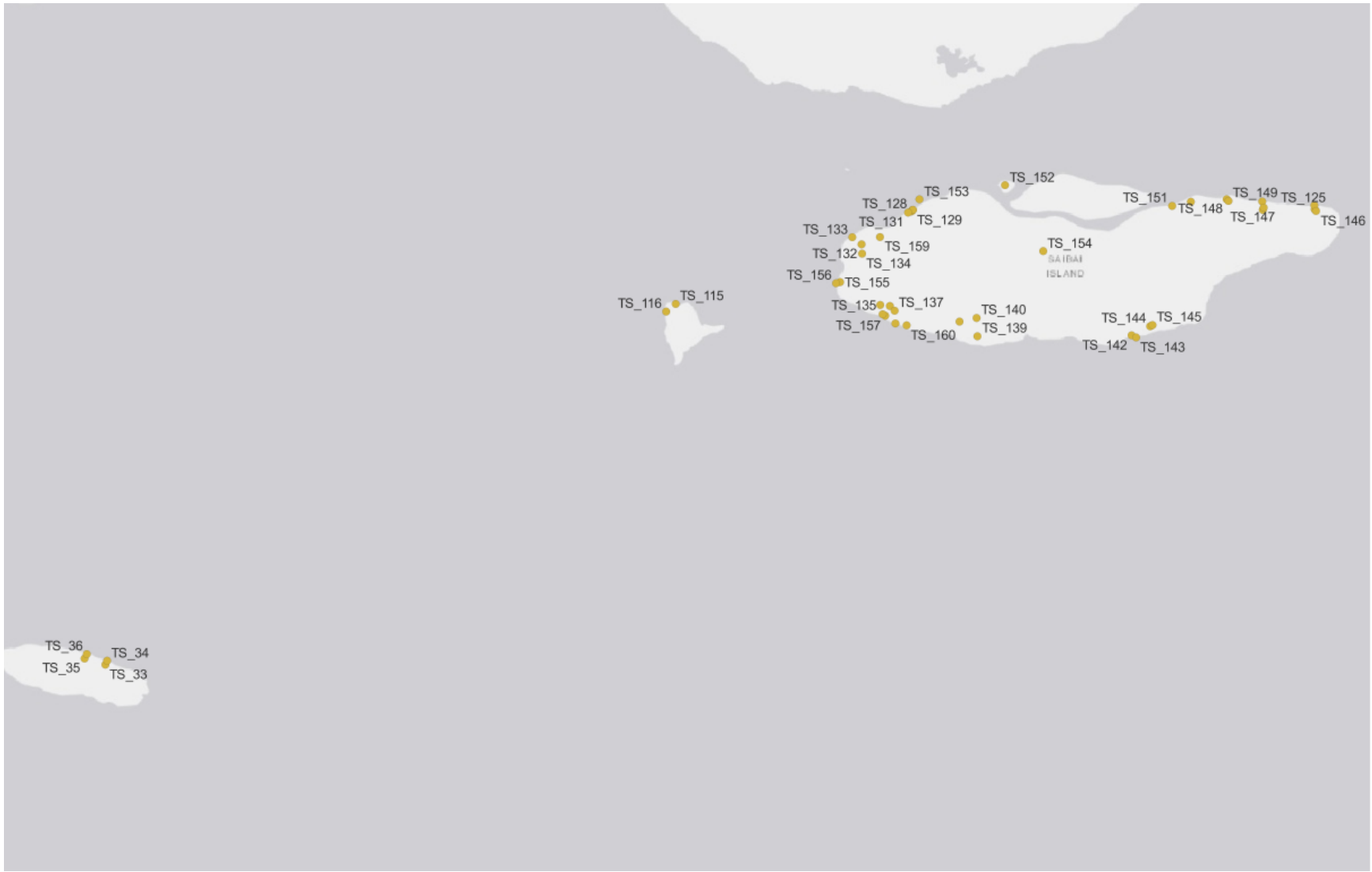

Figure 16. The long-term NDVI sample sites at and around Saibai Island, including Dauan and Turnagain, estimated from Landsat imagery between 1987 and 2021.

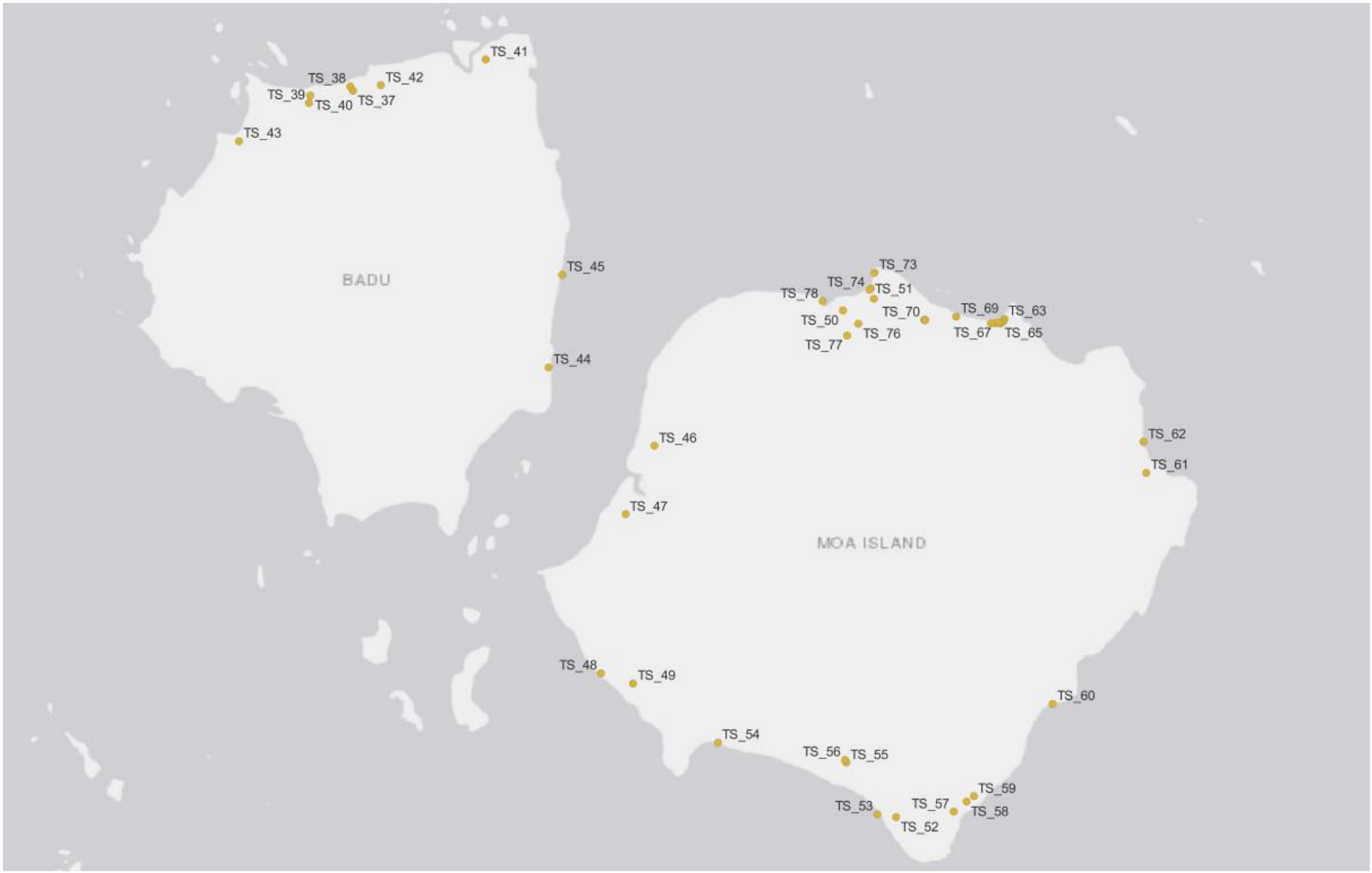

Figure 17. The long-term NDVI sample sites at and around Moa and Badu Islands, estimated from Landsat imagery between 1987 and 2021.

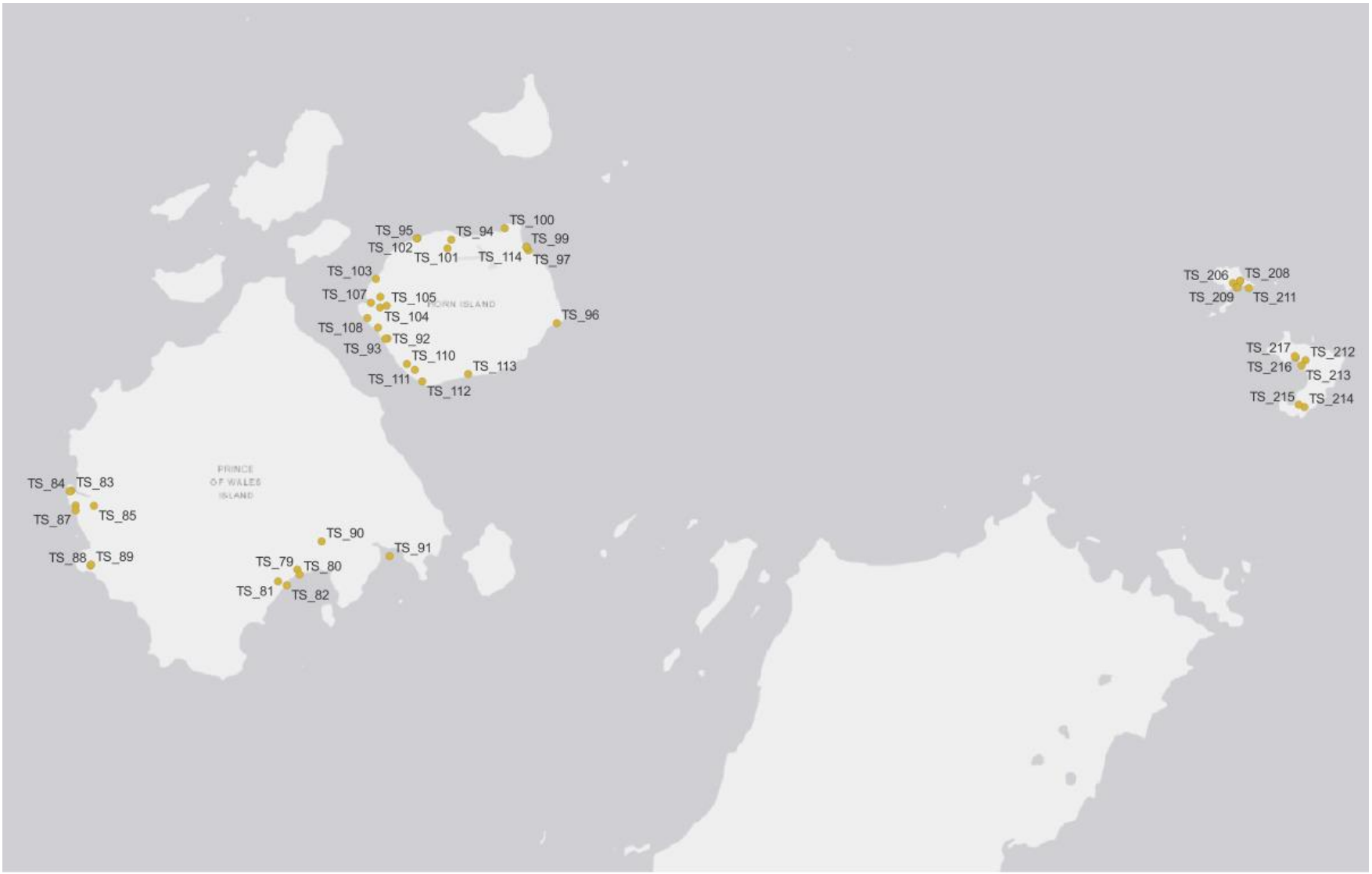

Figure 19. The long-term NDVI sample sites at and around Prince of Wales and Horn Islands, including Little Adolphus and Mori islands, estimated from Landsat imagery between 1987 and 2021.

Root Burial – Storm impacts

Mangroves often have aerial roots that allow respiration to occur in otherwise anoxic wet and saline substrate. However, if aerial roots become buried from sediment deposition, usually from flood and shoreline accretion processes, then mangroves can face reduced vigour or even death (Ellison, 1999). Site TS_68 at Gerain Point on Moa island (Figure 20) exemplifies where root burial appears to have occurred since 2008 from a shifting sand ridge, driving a progressive loss of the seaward zone. Figure 21 photographically exemplifies root burial at McIvor River in East Cape York (Duke and Mackenzie, 2018).

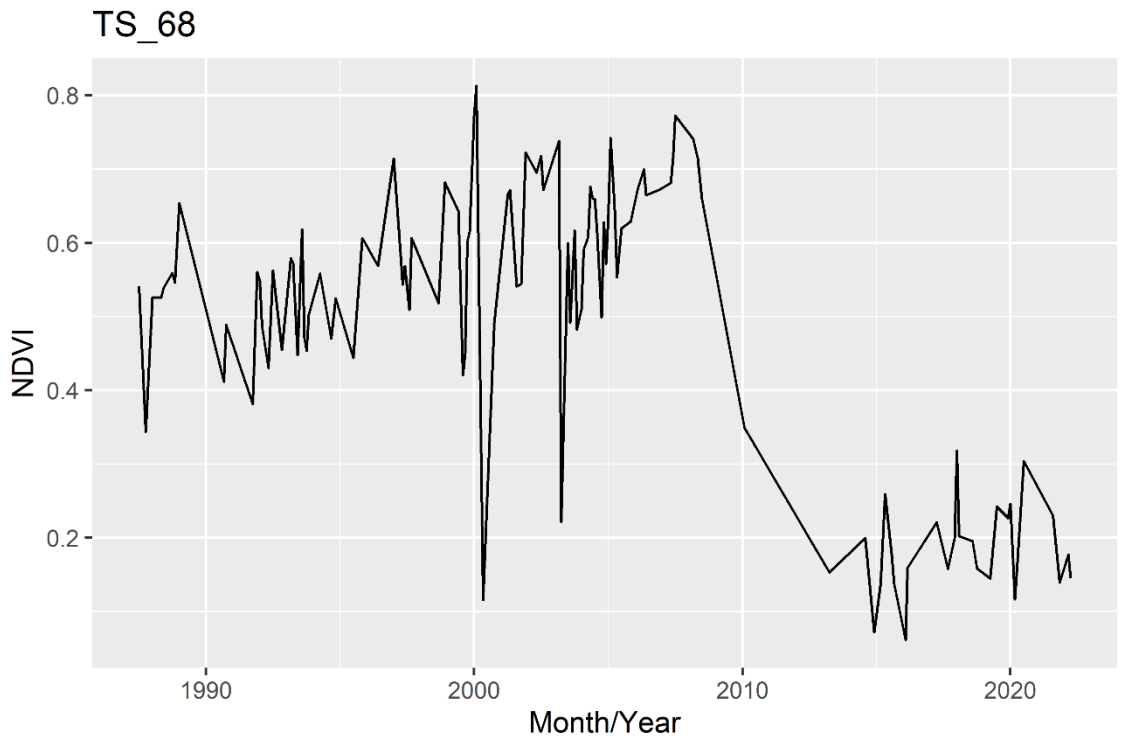

Figure 20. The long-term NDVI at site TS_68 at Gerain Point, Moa Island, estimated from Landsat imagery between 1987 and 2021.

Figure 21. Root burial exemplified at McIvor River in East Cape York (Duke and Mackenzie, 2018).

Lightning Gaps – Storm impacts

Lightning occurs at high frequencies in the tropics, and it can create gaps in forests where lightning strikes alight and incinerate patches of trees (Yanoviak et al., 2020). While a localised disturbance, an analysis of gaps in Moreton Bay, Queensland, observed disturbed patches ranging from 27 m^2 to 474 m^2 (Amir and Duke, 2019). In addition to lightning gaps, forests may experience burning from sporadic or intentional fires, likely yielding a similar impact. Site TS_108 on Horn Island exemplifies an observable drop in canopy condition in 2013, where the ground is visibly blackened in imagery (Figure 22). This appears a blip in the long-term trends, largely attributed to the spatial and temporal scale at which lightning gaps occur. Given that Landsat imagery has a resolution of 25x25m (625 m^2), it is likely that Landsat imagery may be too course to detect many light-gaps, and more resolved imagery would be necessary, such as that from Sentinel satellites (10 m resolution) or shoreline aerial assessments (0.02 m resolution) (Mackenzie et al., 2016). Figure 23 exemplifies a lightning gap at the Gulf of Carpentaria (Duke et al., 2021).

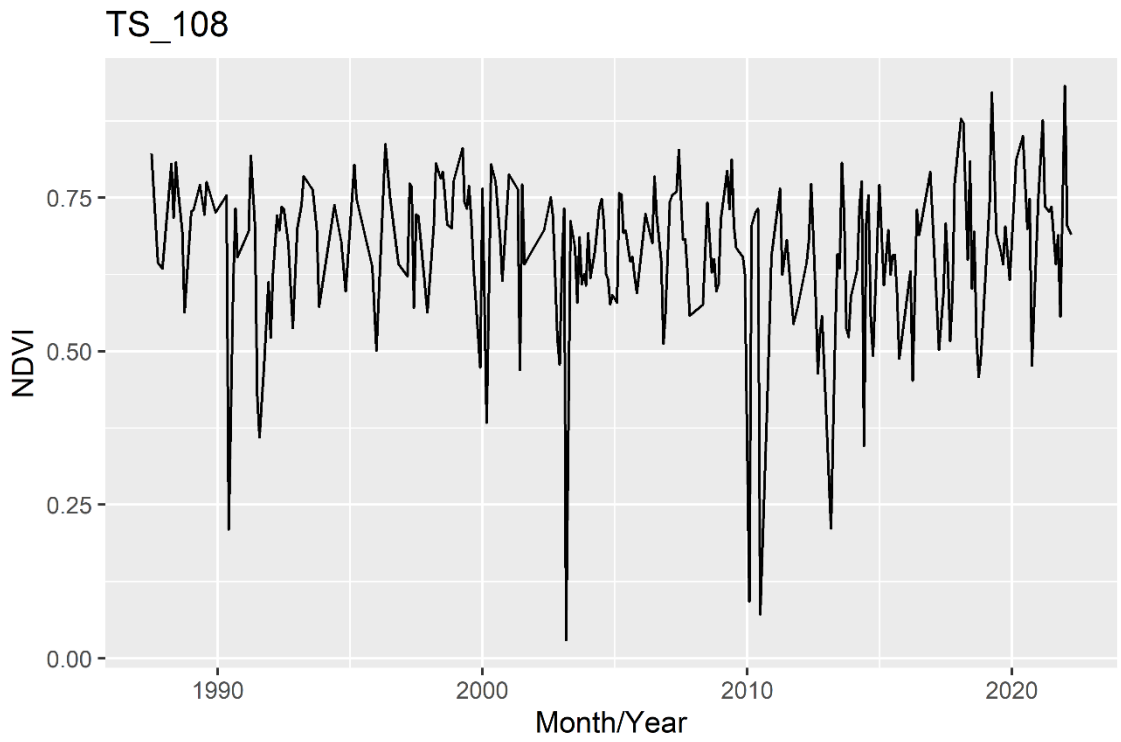

Figure 22. The long-term NDVI at site TS_108 on Horn Island, estimated from Landsat imagery between 1987 and 2021.

Figure 23. Lightning gap exemplified within the Gulf of Carpentaria (Duke et al., 2021).

Depositional Gain – Flooding/Sediment Runoff

Depositional gain occurs when mangrove seedlings and saplings occupy accreting mudbanks exceeding elevations above mean sea level - the mangrove 'sweet spot' zone (Duke et al., 2021). Accreting mudbanks typically arise from the deposition of sediment carried by floodwaters, and are often associated with bank erosion upstream, generally observed in meandering channels. As sediment deposition is often associated with periodic flood events, the expanding vegetation canopy is often stepped and incremental (Duke et al., 2021).

We exemplify this at two sites: (1) TS_87 at the western coast of Prince of Wales island (Figure 24), where gain has occurred from about 2013 onwards (scattered saplings visible since 2003); and (2) TS_190 on Sassie Island (Figure 25), where there has been a steady increase between 1990 and 2015, which was a sandy flat in 1985 and dense saplings in 2016. Figure 26 exemplified depositional gain within the Gulf of Carpentaria (Duke et al., 2021).

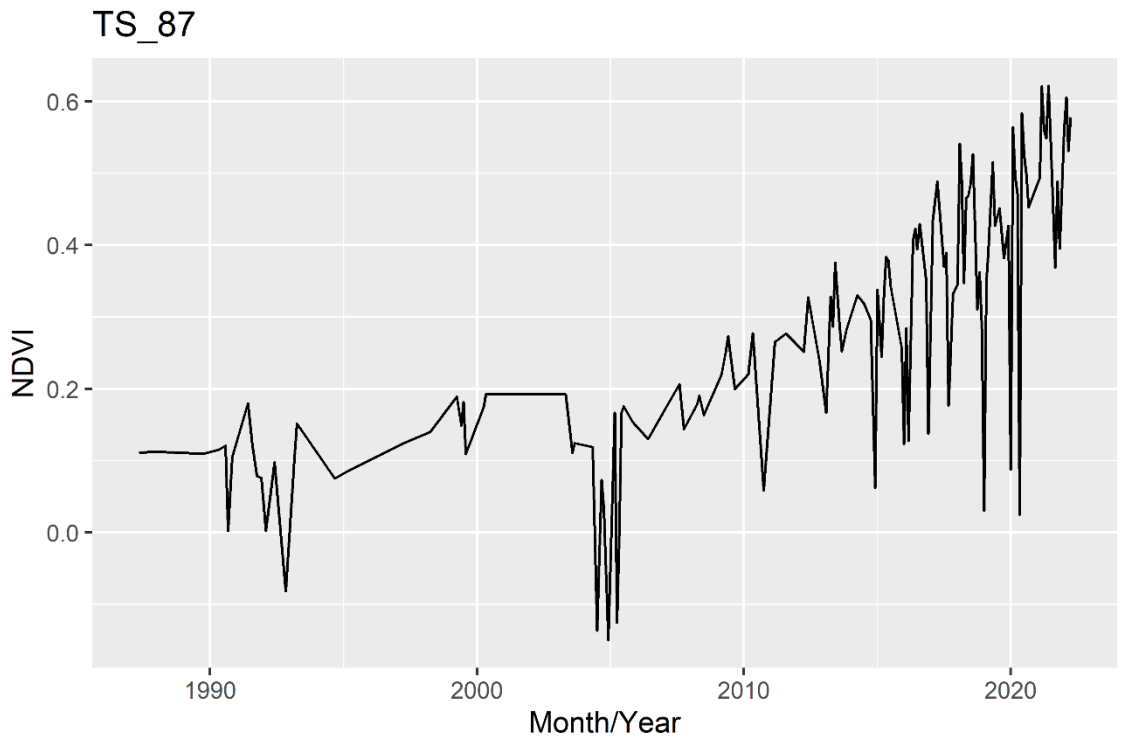

Figure 24. The long-term NDVI at site TS_87 on Prince of Wales island, estimated from Landsat imagery between 1987 and 2021.

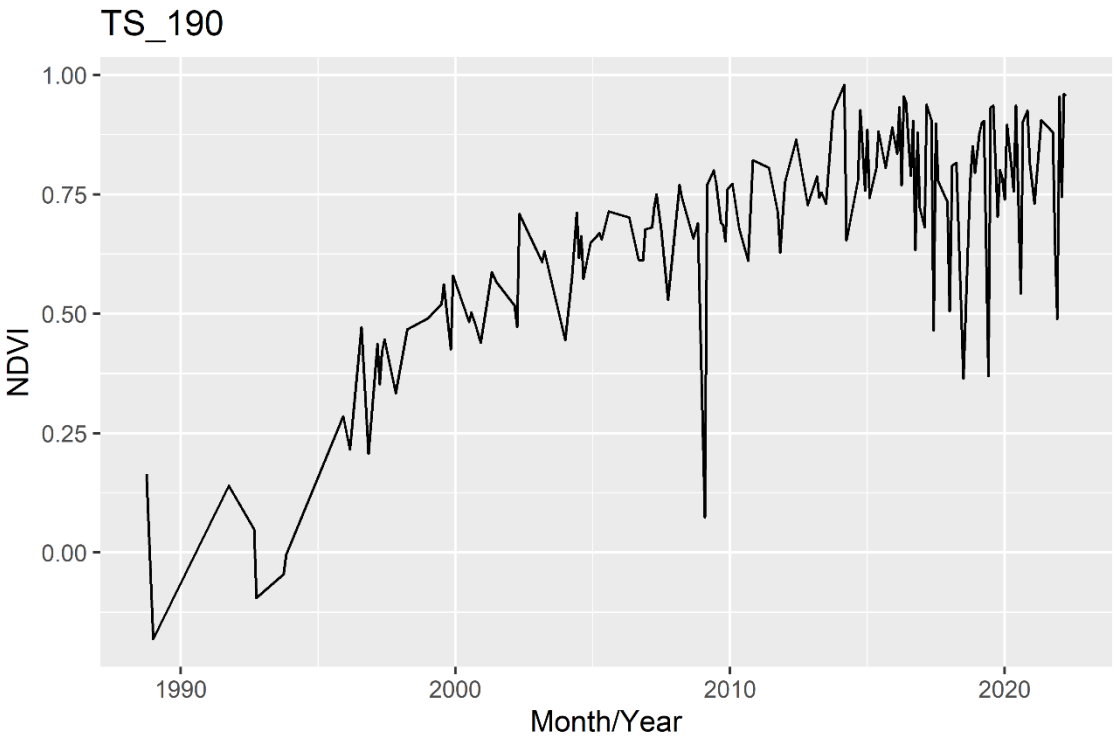

Figure 25. The long-term NDVI at site TS_190 at Sassie island, estimated from Landsat imagery between 1987 and 2021.

Figure 26. Depositional gain exemplified within the Gulf of Carpentaria (Duke et al., 2021).

Ecotone Shifts – Rainfall and sea level rise

An ecotone is a transitional area of vegetation between two different plant communities, such as mangrove forest and saltmarsh. The ecotone between mangrove and saltmarsh communities can shift with changing climatic patterns, for example, sea level rise can lead to increased inundation and mangrove occupation of the landward edge of existing mangrove, shifting the mangrove-saltmarsh ecotone inland (Cavanaugh et al., 2019; Saintilan et al., 2019). Furthermore, Duke et al (2019a) demonstrated a sigmoidal relationship between long-term rainfall and the relative area of mangrove to saltmarsh in estuaries across northern Australia. Accordingly, long-term increases in rainfall are predicted to increase the encroachment of mangrove onto saltmarsh, while decreases in rainfall are predicted to cause mangrove dieback and an expansion of saltmarsh – ecotones shifting accordingly (Duke et al., 2019).

This is exemplified at TS_77 on Moa Island (Figure 27), where sea level rise has driven a progressive upward shift of the upper ecotone. Figure 28 exemplifies an ecotone shift occurring at Harmer River in East Cape York (Duke and Mackenzie, 2018).

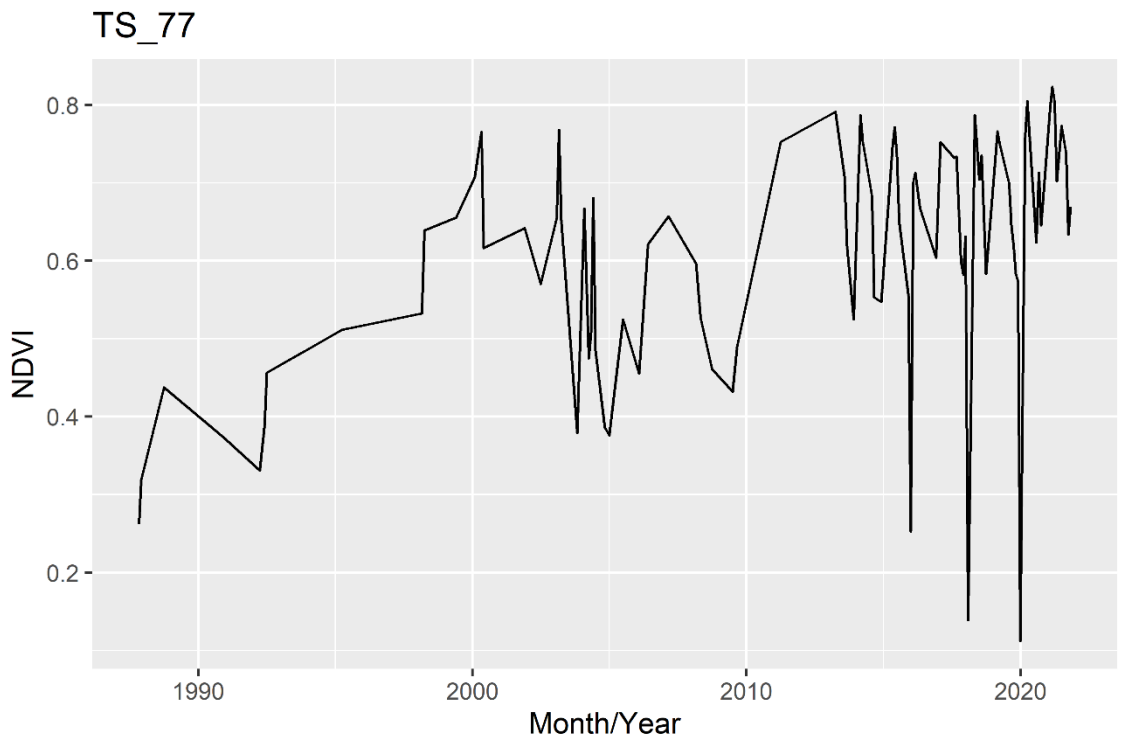

Figure 27. The long-term NDVI at site TS_77 on Moa Island, estimated from Landsat imagery between 1987 and 2021.

Figure 28. Ecotone shift exemplified at Harmer River in East Cape York (Duke and Mackenzie, 2018)

Cyclone damage – Storm impacts

Mangroves provide coastal protection through surge and wind suppression during tropical cyclones, and are generally resilience to the wind effects of cyclones unless another environmental change has also occurred, such as hydrological alteration or sedimentation, or legacies from previous disturbances are reducing resilience (Krauss and Osland, 2020). For example, Tropical Cyclone Yasi (category 5), caused severe windthrow (winds exceeding 280 km/h) to an estimated 13,795 ha of mangroves within and surrounding Hinchinbrook Island National Park. In this instance, recovery was poor due to the inability of the dominant species (*Rhizophora stylosa*) to resprout from remaining plant material and due to increased sea inundation driven by a reduction in sediment elevation (Asbridge et al., 2018).

Tropical cyclones are rare in the Torres Straits region (Figure 29; Table 2), though there is large uncertainty about how tropical cyclone behaviour may change with climate change. Solomon et al (2007) reported that intensity of tropical cyclones will increase globally under climate change, but a lack of regionally specific information means it is difficult to state how any change in tropical cyclone activity may impact the Torres Strait Region (Green et al., 2009). We did not readily observe cyclone damage at any of the sample locations, though cyclone damage may become an additional stressor with climate change, and post-cyclone monitoring is recommended should they occur in the region.

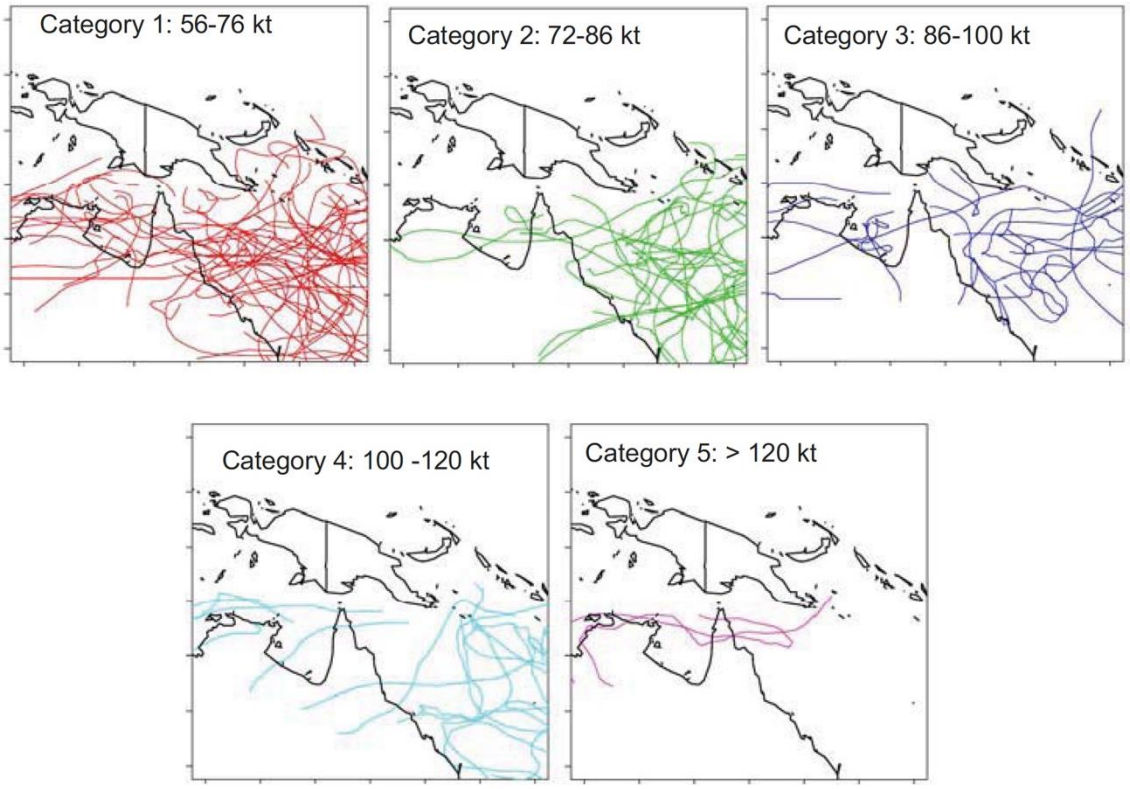

Figure 29. Tropical cyclone tracks of Category 1 to 5 that occurred over northeast Queensland and the vicinity of the Torres Strait region between 1969-2018. Source: US National Climatic Data Center, Ashville.

Table 1. The date, name, magnitude category (cat.), direction, pressure (press.), and likely location of cyclones observed in the vicinity of Torres Straits.

Year	Date	Name	Cat.	Direction	Press.
1920	17 Dec	AU192021_01U			
1923	25 Mar	AU192223_08U	3		985
1948	6 Jan	AU194748_02U			989
1953	14 Apr	AU195253_09U			1003
1957	11 Apr	AU195657_02U	1		1002
1964	6 Jan	Audrey	5		1000
1972	22 April	Faith		west	997
1979	7 April	Stan	4	west	1003
1998	20 Mar	Nathan	1		990
2003	16 Dec	Jana	1		1005
2004	12 Mar	Fay	1	west	1006
2005	14 Apr	AU200405_01U			995
2006	22 Feb	Kate		east	1000
2007	21 May	Pierre	1	west	1007
2007	19 Nov	Guba			990

Figure 30. Cyclone damage exemplified within the Gulf of Carpentaria (Duke et al., 2021).

Shoreline Retreat and Terrestrial Retreat – Sea level rise

As the planet warms from excessive greenhouse gas emissions, Earth's ice caps at the north and south pole melt and the ocean expands, this leads to sea level rise. As a result, low lying coastal and island areas, such as those across the Torres Straits, become increasingly vulnerable to submersion(Green et al., 2009). Mangrove forests and salt marsh typically occupy the coastal zone between the mean sea level height and the high tide height, with the proportion of mangrove coverage to salt marsh increasing with long-term rainfall (Duke et al., 2019). As sea level rises, the seaward mangrove fringe becomes excessively submerged, or drowns, causing dieback known as 'inner fringe collapse' and shoreline retreat (Duke et al., 2021). While landward fringes are expected to expand inland (terrestrial retreat) if the land profile allows the high tide inundation extent to increase.

Shoreline retreat can be exemplified at TS_142 on Saibai island (Figure 31), where canopy condition has been steadily declining since 2000. Figures 32 and 33 exemplify shoreline retreat and terrestrial retreat within the Gulf of Carpentaria (Duke et al., 2021).

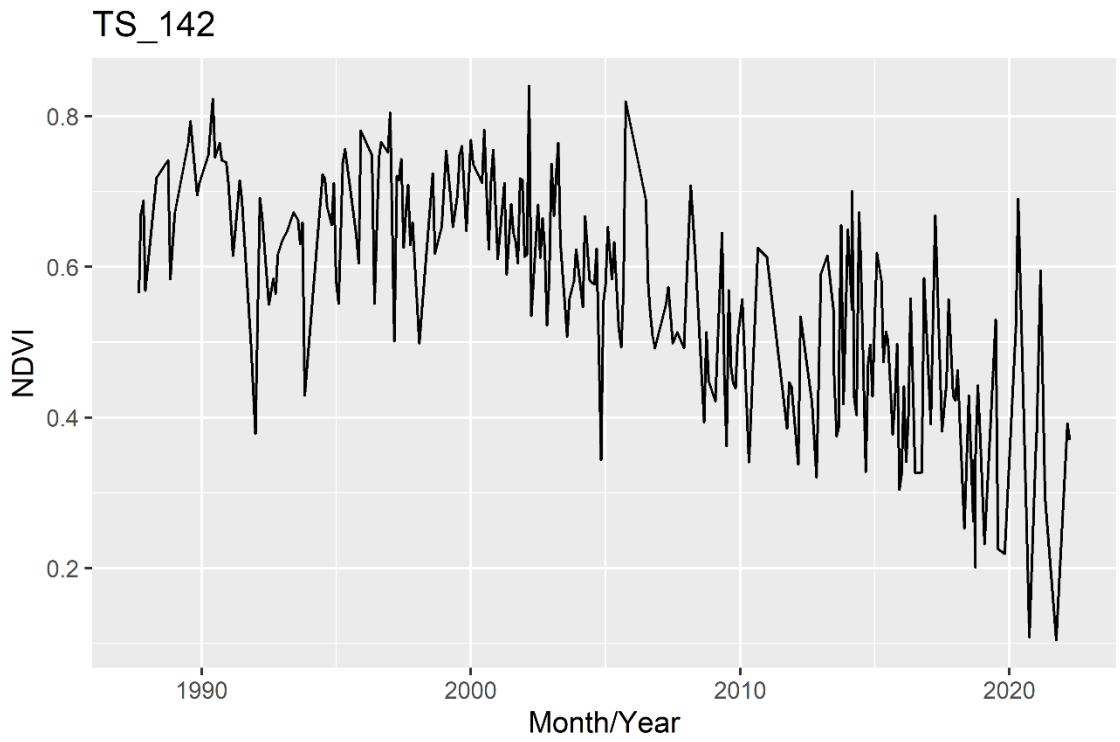

Figure 31. The long-term NDVI at site TS_142 on Saibai Island, estimated from Landsat imagery between 1987 and 2021.

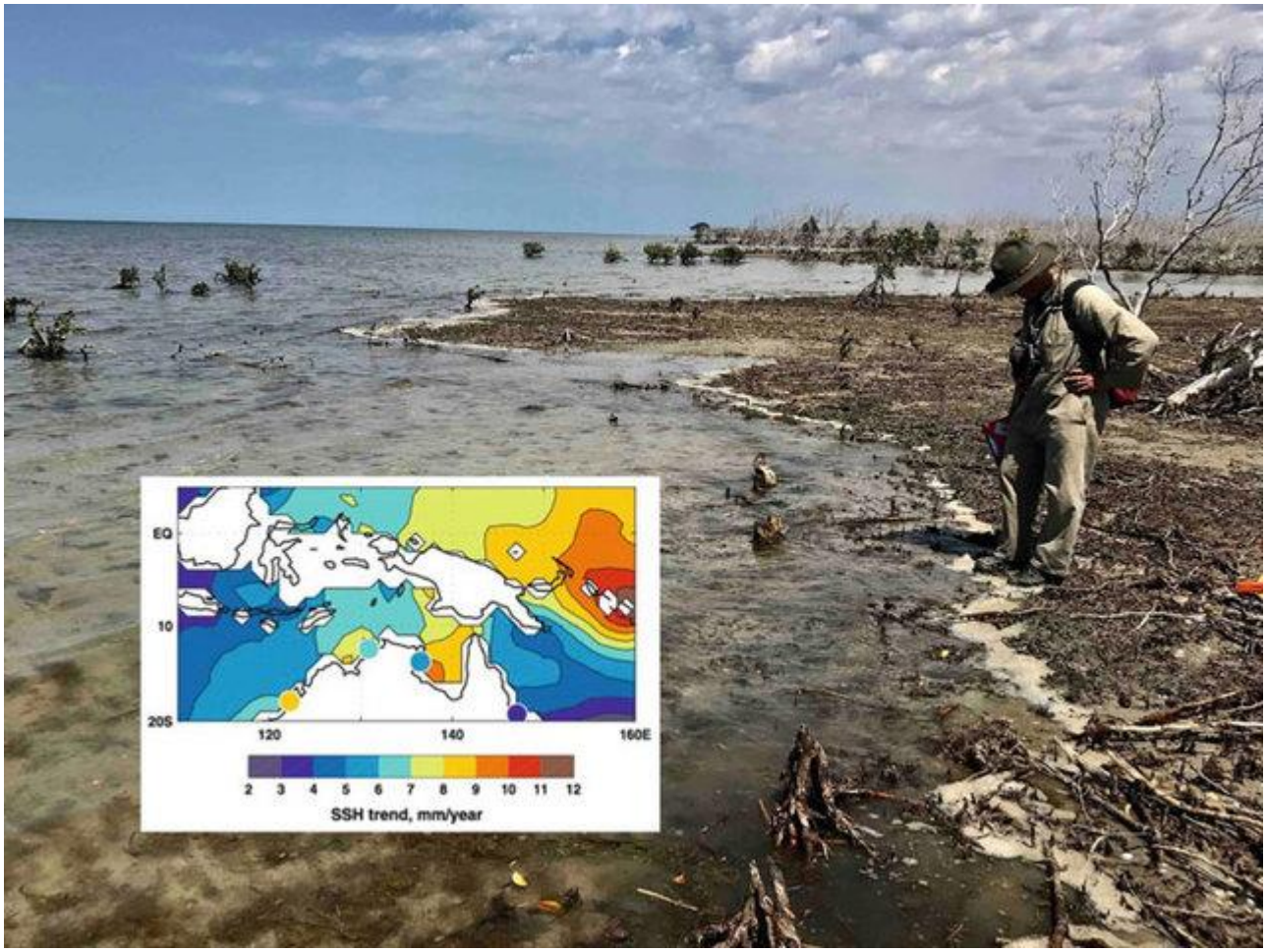

Figure 32. Shoreline retreat exemplified within the Gulf of Carpentaria (Duke et al., 2021).

Figure 33. Terrestrial retreat exemplified within the Gulf of Carpentaria (Duke et al., 2021).

Sea level oscillations – Climate change

The Torres Strait islands are also exposed to changes in sea level driven by the El Niño–Southern Oscillation (ENSO), which is an irregular periodic variation in winds and sea surface temperatures over the tropical eastern Pacific Ocean, oscillating between El Niño and La Niña states. In contrast to El Niño states, La Niña states typically results in increased rainfall, warmer overnight temperatures, earlier monsoon onset and a greater number of tropical cyclones. ENSO events typically occur over approximately six months every 5-10 years, impacting regional sea levels by ~20-30 cm, with lower than average sea level occurring during El Niño and higher than average occurring during La Niña (Becker et al., 2012; Miles et al., 2014; Piecuch and Quinn, 2016).

Given that mangroves can use both fresh and saline waters for hydration (Reef and Lovelock, 2015; Santini et al., 2015), the low sea levels and drought conditions brought about during El Niño can cause desiccation dieback (Lovelock et al., 2017; Duke et al., 2022). Large scale desiccation dieback events (~80 km^2), coinciding with El Niño, have occurred in 1982 and 2015 across Australia's Gulf of Carpenteria (Duke et al., 2022), and it is plausible that these events have caused dieback in other locations experiencing similar conditions. Furthermore, given the periodic nature of ENSO, it is likely similar diebacks will occur in the future, and potentially more frequently given a changing climate. Examining these events revealed that mangroves likely have an annual fluctuation in canopy cover, driven by seasonal sea level changes, and an inter-decadal fluctuation where forests may be heavily disturbed by desiccation during extreme low sea levels or drowning during extreme high sea levels, as depicted in Figure 34.

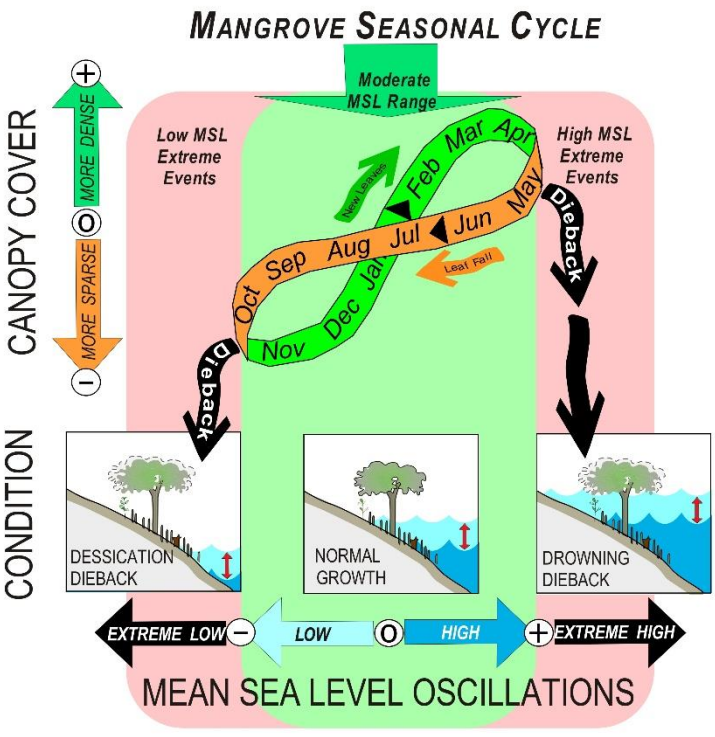

Figure 34. The relationships between canopy condition of tropical, semi-arid shoreline mangroves and mean sea level (MSL) identified during this study. When conditions exceeded the mangrove Goldilocks zone (central green shaded block) of normally moderate annual oscillations in mean sea level, severe destructive impacts occurred as a result of high or low extreme events (drowning or desiccation dieback respectively; pink shaded blocks). Moderate oscillations appear to drive natural seasonal cycles of leafing and leaf fall where low levels (less inundation) correspond with leaf fall (maximal in Sept-Nov), and high levels (more inundation) with new leaf production (maximal in Mar-May).

Figure and caption reproduced from:

Duke, N., Mackenzie, J., Canning, A., Hutley, L., Bourke, A., Kovacs, J., Cormier, R., Staben, G., Lymburner, L., & Ai, E. (2022). ENSO-driven extreme oscillations in mean sea level destabilise critical shoreline mangroves - an emerging threat. *In Review at PLOS Climate*.

From our analysis, we suspect site TS_49 on Badu island (Figure 35) experienced a reduction in canopy condition coinciding with the El Niño driven extreme reductions in sea level and low rainfall in 2015 (known by the Samoan term 'Taimasa').

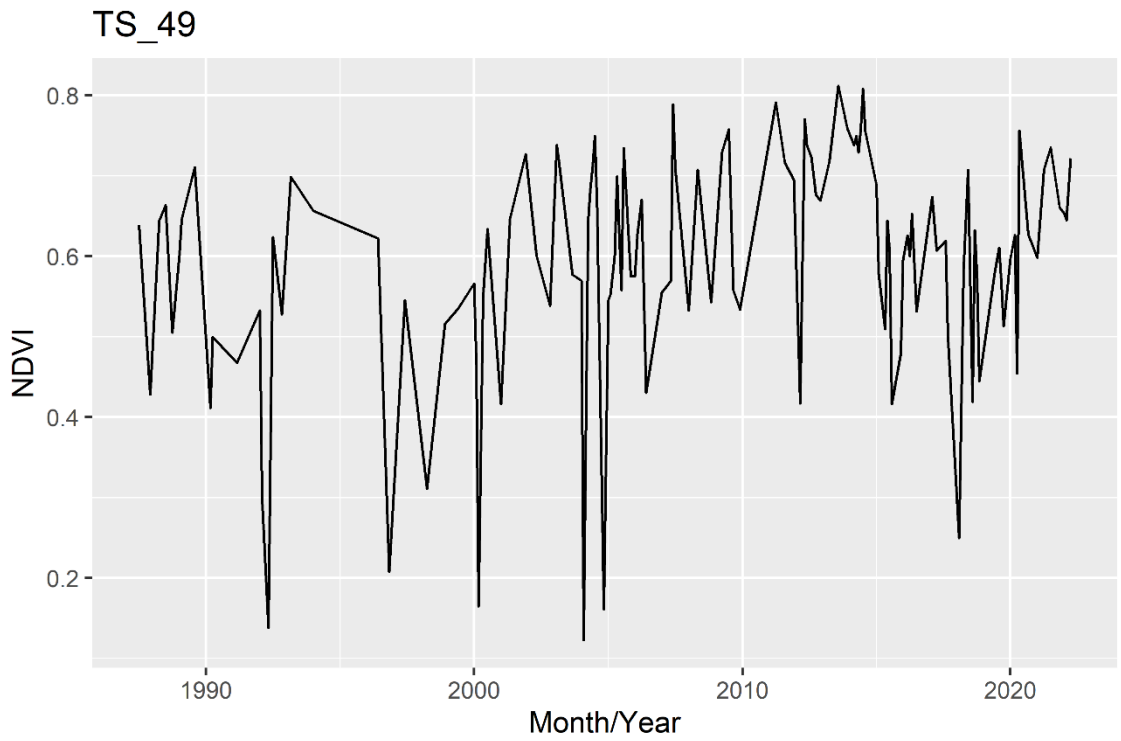

Figure 35. The long-term NDVI at site TS_49 on Badu Island, estimated from Landsat imagery between 1987 and 2021.

In addition to the drop in canopy condition exemplified at TS_49, we further exemplify the climatic oscillations in canopy condition via the following:

1. Figure 36 shows locations at Prince of Wales and Horn Islands, positioned at the front and back edges of the shoreline mangrove zone. These sites were chosen as they were closest to the tide gauge. The observation here is that sites at both the front and back edge generally follow the same patterns in canopy condition, suggesting they are responding to the same or similar influences.
2. When the sites at the front edge and back edge are averaged together, the oscillation in canopy condition corresponds significantly to oscillations in sea level. This is shown in Figure 37, where the rolling six-month anomaly (also known as the 'sea level stress index', (Duke et al., 2022)) is compared with the rolling six month anomaly of the NDVI (canopy condition index). For the sea level stress index, significant canopy stress and dieback typically occur between values of +/- 300-400 (Duke et al., 2022), and these are indicated on Figure 29.
3. Finally, for each month, we calculated the difference in NDVI score of a 12-month rolling window (six months either side) to indicate the magnitude of change occurring over a given period. We then correlated the change in canopy condition with the sea level stress index at the time (Figure 38). These were well correlated, particularly at the back edge sites where approximately half of the variation was explained by the sea level stress index.

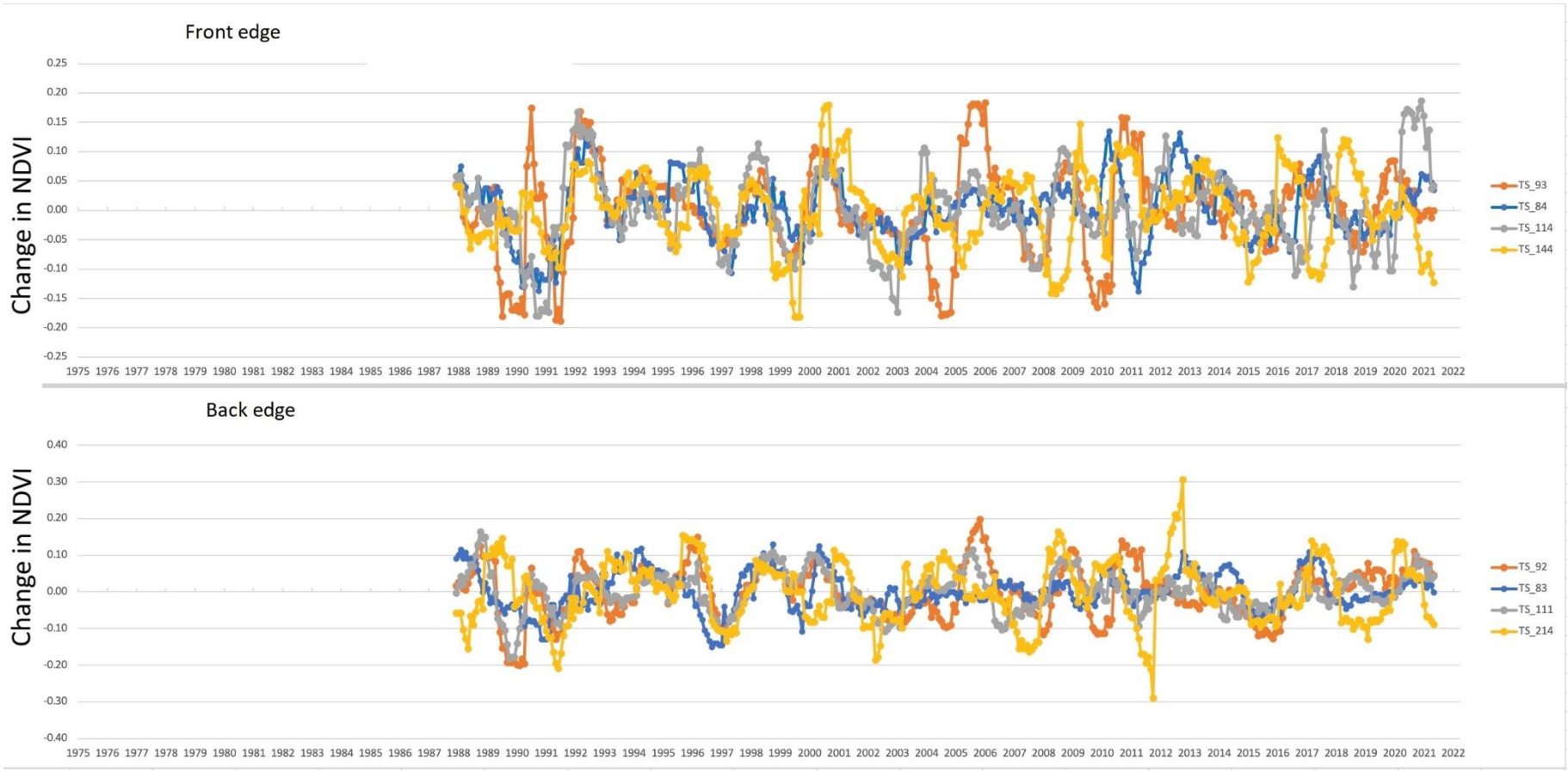

Figure 36. The rolling twelve month difference in NDVI scores (six months before and six months after the displayed date) at four sites at front edge and four sites at the back edge of mangroves at the shoreline zone on Prince of Wales and Horn Islands.

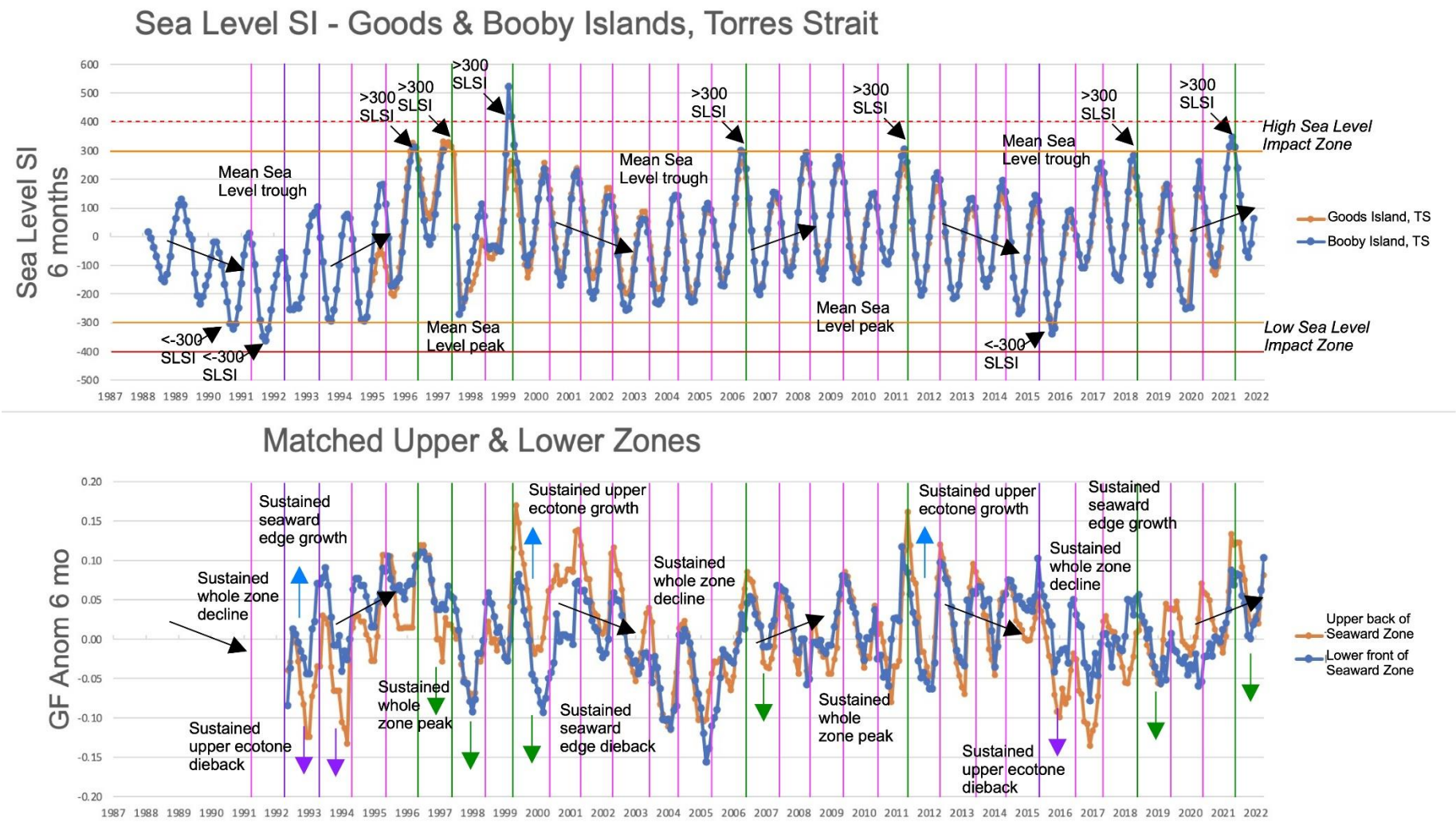

Figure 37. (Top) The rolling six-month anomaly (also known as the 'sea level stress index', (Duke et al., 2022)); (Bottom) The rolling six month anomaly of the NDVI (canopy condition index). Significant canopy stress and dieback typically occur with SLSI values between +/- 300-400 (Duke et al., 2022),

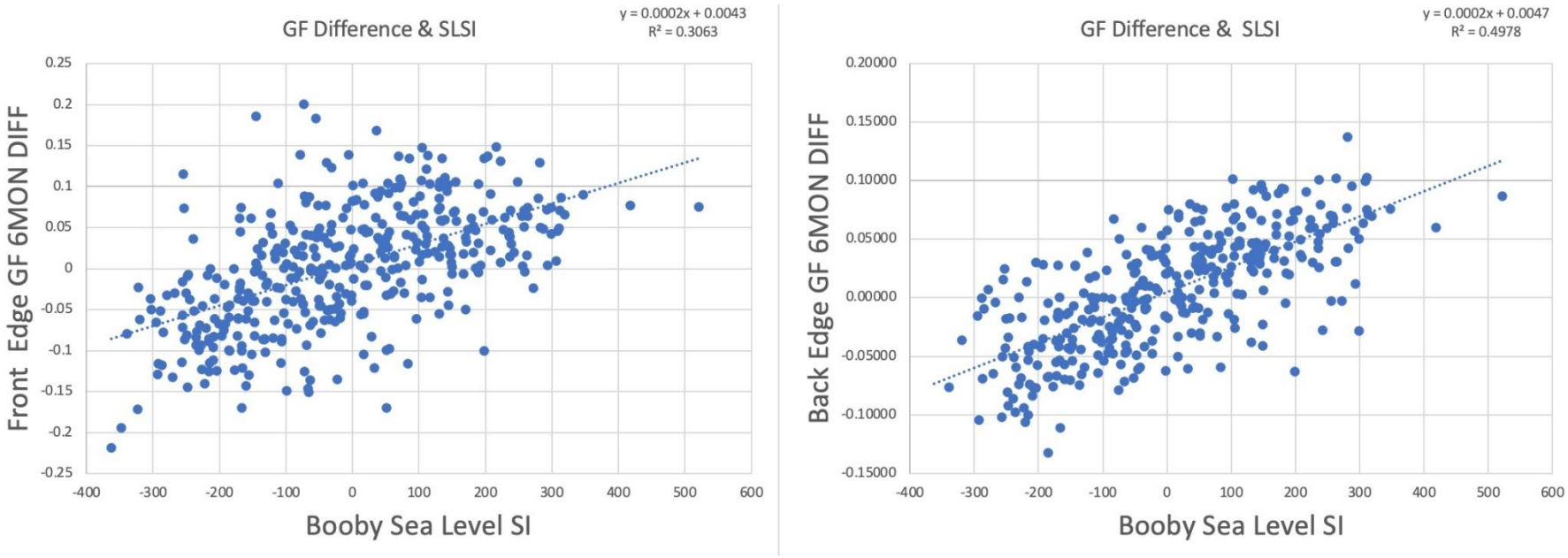

Figure 38. Correlation of the difference in NDVI score of a 12-month rolling window (six months either side) versus the sea level stress index at front edge (left) and the back edge (right) at eight sites across mangroves at the shoreline zone on Prince of Wales and Horn Islands.

Mangrove clearing - Harvesting

In the Torres Straits, mangroves are subject to direct removal to clear land for occupation and as a source of timber or fuel (Duke et al., 2015). While forests are likely resilient to some harvesting, over-harvesting can reduce the ability of forests to recover and result in localised collapse (Fontalvo-Herazo et al., 2011).

Our analysis did not readily observe any decline from mangrove harvesting; however, the authors have limited knowledge on what areas are heavily harvested, and the Landsat imagery resolution of 25x25m (625 m^2) is likely too course to detect small scale harvests. As with detecting light-gaps, more resolved imagery would be necessary, such as that from Sentinel satellites (10 m resolution) or shoreline aerial assessments (0.02 m resolution) (Mackenzie et al., 2016).

We did, however, observe unusually excessive depositional gain occurring at TS_171 on Iama island (Figure 39), which we suspect is resultant of sediment deposition from upstream bank erosion caused by harvesting, showing that impacts of harvesting are not always localised.

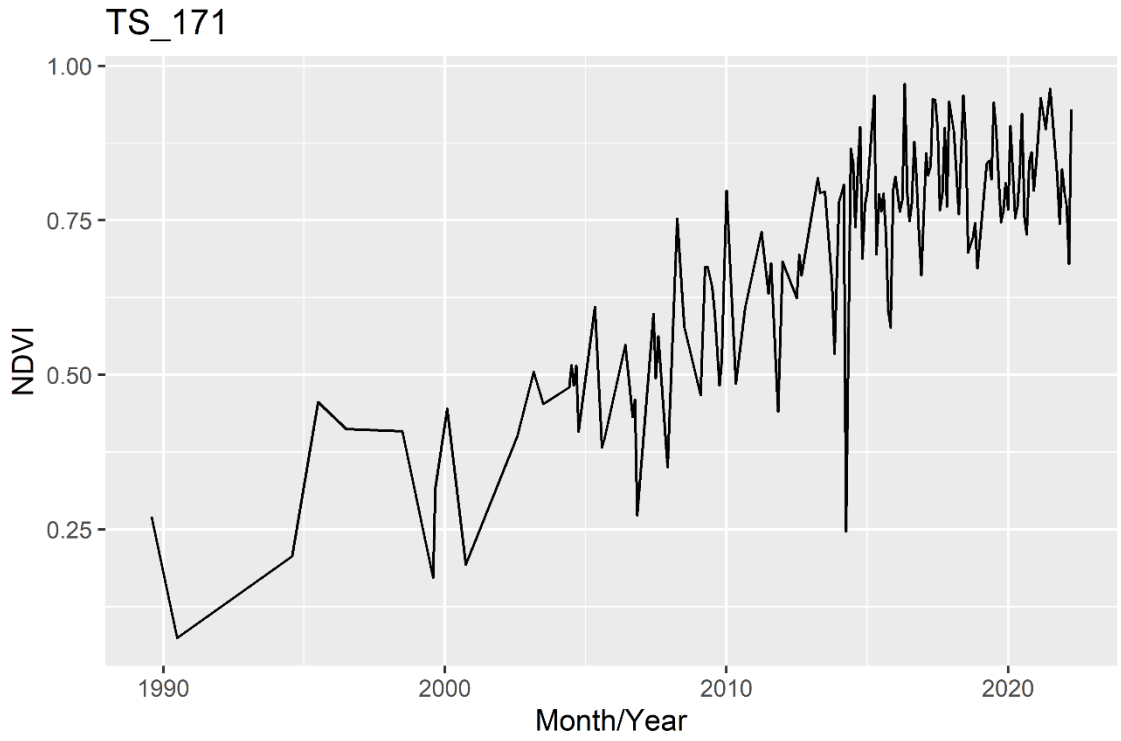

Figure 39. The long-term NDVI at site TS_171 on Iama Island, estimated from Landsat imagery between 1987 and 2021.

Fire damage

Like their terrestrial counterparts, mangrove forests can also suffer from bush fires. While mangroves experience regular tidal inundation and do not have the same mass of dry leaf litter accumulation that terrestrial forests, fires can still occur in the canopy, and they can still experience heat stress from nearby fires. Evidence of fire damage is exemplified at TS_70 on Moa island, where the ground appears blackened with a sharp drop in canopy condition in December 2006 (Figure 40).

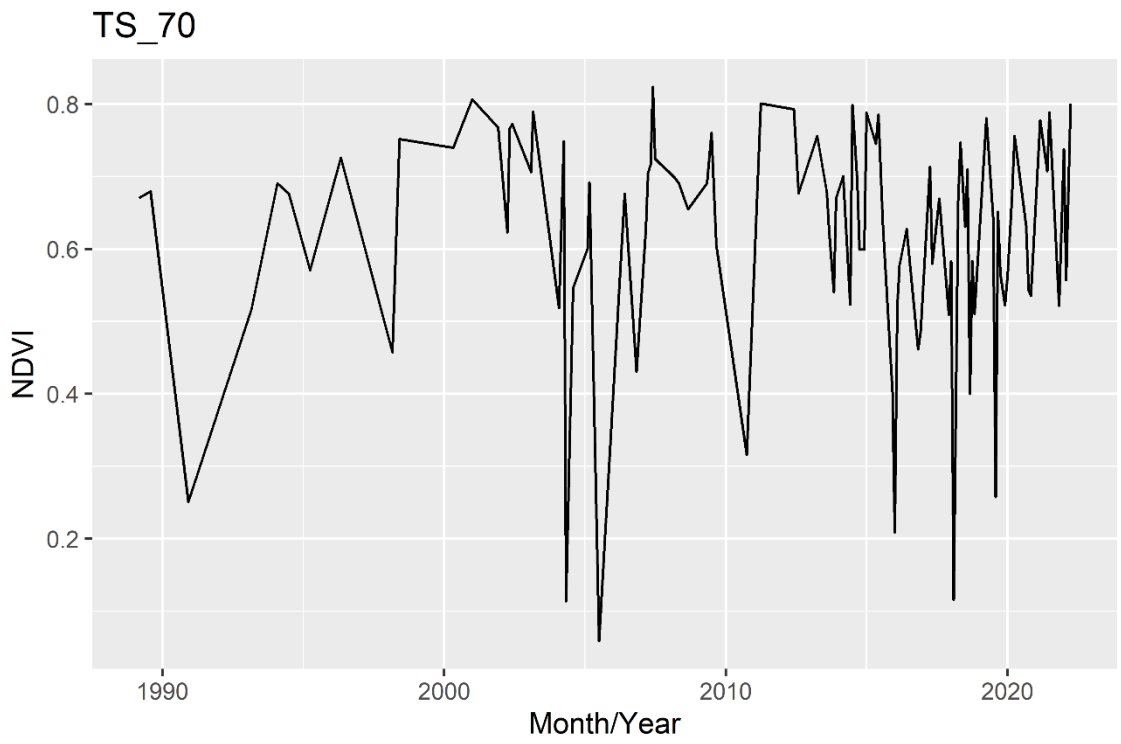

Figure 40. The long-term NDVI at site TS_70 on Moa Island, estimated from Landsat imagery between 1987 and 2021.

Recommendations

Given the expansiveness of mangroves across the Torres Straits, we suggest that a long-term monitoring program utilise satellite remote sensing to capture monthly and annual changes that are also coupled with in-field shoreline surveys that are repeated on a 5-10 year cycle. The remote sensing data indicators could then alert where management actions/interventions are required to assess and potentially remedy any areas of concern (or "alert to action"). This monitoring program would involve training rangers and support them in making more informed management decisions. Furthermore, it would support and validate state of environment assessments (TSRA, 2021). Establishing this monitoring program would involve several steps:

1. Carry out a baseline survey of all mangroves across the Torres Straits using helicopter-based shoreline imagery, such as that described in Mackenzie et al (2016) and partially completed in parts of the Torres Strait by Duke et al (2015). This process involves taking high-resolution oblique imagery of the entire mangrove extent, calculating scores for a suite of mangrove health indicators, interpreting observations and likely drivers, then developing locally-specific recommendations for management. This information could be presented as a series of local report cards, such as that in Appendix B. Note: Appendix B is an example from the Queensland's Endeavour River of where the method has been previously applied and is not indicative of mangroves in the Torres Strait. The shoreline surveys not only provide a permanent record for establishing long-term change, but they allow for the identification of stressors and potentially sensitive areas where frequent remote sensing monitoring should be targeted.
2. Use remote sensing, such as that exemplified in this report, to monitor locations across mangroves spanning the entire Torres Straits. Sites used in this assessment would need to at least cover all stressed and potentially stressed sites, sites with very low to no stress, and any sites of cultural or other special significance. At these sites, monitoring should occur at points over transects spanning between the seaward edge to the landward edge, allowing greater detection of ecotone shifts. Data obtained from remote sensing should indicate on canopy condition (such as that shown in this report) and estimate extent of all tidal ecosystems (including mangrove forest and saltmarsh-saltpan) to calculate the Wetland Cover Index (Duke et al., 2019). The Wetland Cover Index typically corresponds to long-term rainfall; however, if the index changes and there is no discernible change in rainfall then that signals a need for further investigation. Any follow up investigation should aim to quantify the severity, duration and extent of the stress, as well as the driver and potential management interventions. The results of remote sensing data could inform an annual assessment report, with a short list of important or sensitive sites potentially presented monthly via an online dashboard that triggers more responsive action.
3. In establishing (2), it would be necessary to ground truth patterns observed in remote-sensing with local mangrove processes. To do this, we suggest carrying out an 18 month (approximately) study at a range of selected sites to assess:
    a. The mangrove forest seasonal pulse rates by estimating leaf litter fall and shoot-counts.
    b. Canopy coverage using photography and/or light meter readings to estimate the Leaf Area Index.
    c. The movement of infauna (such as crabs) and leaf litter on the ground using short-term video or timelapse photography of quadrats.

4. Establish long-term monitoring plots to assess changes in the stand species composition, structure, biomass, and demography. This would involve identifying plot locations, tagging trees, measuring stem diameter, tree height, tree coordinates, and seedling quadrants. Trees would then be re-assessed every five years.
5. Establish long-term tide gauges and weather monitoring sites at locations that indicate conditions experienced in the northern, central and eastern islands. Current monitoring is focussed on the southern islands. There used to be monitoring occurring at Daru; however, we were unable to source data from this location and it needs investigating whether this monitoring still occurs and the data availability.

References

Amir, A. A., and Duke, N. C. (2019). Distinct characteristics of canopy gaps in the subtropical mangroves of Moreton Bay, Australia. *Estuarine, Coastal and Shelf Science* 222, 66–80. doi: 10.1016/J.ECSS.2019.04.007.

Asbridge, E., Lucas, R., Rogers, K., and Accad, A. (2018). The extent of mangrove change and potential for recovery following severe Tropical Cyclone Yasi, Hinchinbrook Island, Queensland, Australia. *Ecology and Evolution* 8, 10416–10434. doi: 10.1002/ECE3.4485.

Becker, M., Meyssignac, B., Letetrel, C., Llovel, W., Cazenave, A., and Delcroix, T. (2012). Sea level variations at tropical Pacific islands since 1950. *Global and Planetary Change* 80–81, 85–98. doi: 10.1016/J.GLOPLACHA.2011.09.004.

Bishop-Taylor, R., Nanson, R., Sagar, S., and Lymburner, L. (2021a). Mapping Australia's dynamic coastline at mean sea level using three decades of Landsat imagery. *Remote Sensing of Environment* 267, 112734. doi: 10.1016/J.RSE.2021.112734.

Bishop-Taylor, R., Nanson, R., Sagar, S., and Lymburner, L. (2021b). Mapping Australia's dynamic coastline at mean sea level using three decades of Landsat imagery. *Remote Sensing of Environment* 267, 112734. doi: 10.1016/J.RSE.2021.112734.

Cavanaugh, K. C., Dangremond, E. M., Doughty, C. L., Park Williams, A., Parker, J. D., Hayes, M. A., et al. (2019). Climate-driven regime shifts in a mangrove–salt marsh ecotone over the past 250 years. *Proc Natl Acad Sci U S A* 116, 21602–21608. doi: 10.1073/PNAS.1902181116/SUPPL_FILE/PNAS.1902181116.SAPP.PDF.

Chow, J. (2017). Mangrove management for climate change adaptation and sustainable development in coastal zones. *https://doi-org.elibrary.jcu.edu.au/10.1080/10549811.2017.1339615* 37, 139–156. doi: 10.1080/10549811.2017.1339615.

Duke, N. C., Burrows, D., and Mackenzie, J. (2015). Mangrove and Freshwater Wetland Habitat Status of the Torres Strait Islands. *Biodiversity, Biomass and Changing Condition of Wetlands. Report to the National Environmental Research Program. Reef and Rainforest Research Centre Limited, Cairns (100 pp)*.

Duke, N. C., Field, C., Mackenzie, J. R., Meynecke, J.-O., Wood, A. L., Duke, N. C., et al. (2019). Rainfall and its possible hysteresis effect on the proportional cover of tropical tidal-wetland mangroves and saltmarsh–saltpans. *Marine and Freshwater Research* 70, 1047–1055. doi: 10.1071/MF18321.

Duke, N. C., Hutley, L. B., Mackenzie, J. R., Burrows, D., Duke, N. C., Mackenzie, J. R., et al. (2021). Processes and Factors Driving Change in Mangrove Forests: An Evaluation Based on the Mass Dieback Event in Australia's Gulf of Carpentaria. 221–264. doi: 10.1007/978-3-030-71330-0_9.

Duke, N., and Mackenzie, J. (2018). East Cape York shoreline environmental surveys. Townsville, Australia.

Duke, N., Mackenzie, J., Canning, A., Hutley, L., Bourke, A., Kovacs, J., et al. (2022). ENSO-driven extreme oscillations in mean sea level destabilise critical shoreline mangroves - an emerging threat. *In review at PLOS Climate*.

Ellison, J. C. (1999). Impacts of Sediment Burial on Mangroves. *Marine Pollution Bulletin* 37, 420–426. doi: 10.1016/S0025-326X(98)00122-2.

Fontalvo-Herazo, M. L., Piou, C., Vogt, J., Saint-Paul, U., and Berger, U. (2011). Simulating harvesting scenarios towards the sustainable use of mangrove forest plantations. *Wetlands Ecology and Management* 19, 397–407. doi: 10.1007/S11273-011-9224-4/FIGURES/5.

Gilman, E. L., Ellison, J., Duke, N. C., and Field, C. (2008). Threats to mangroves from climate change and adaptation options: A review. *Aquatic Botany* 89, 237–250. doi: 10.1016/J.AQUABOT.2007.12.009.

Goldberg, L., Lagomasino, D., Thomas, N., and Fatoyinbo, T. (2020). Global declines in human-driven mangrove loss. *Global Change Biology* 26, 5844–5855. doi: 10.1111/GCB.15275.

Green, D., Alexander, L., Mclnnes, K., Church, J., Nicholls, N., and White, N. (2009). An assessment of climate change impacts and adaptation for the Torres Strait Islands, Australia. *Climatic Change 2009 102:3* 102, 405–433. doi: 10.1007/S10584-009-9756-2.

Krauss, K. W., and Osland, M. J. (2020). Tropical cyclones and the organization of mangrove forests: a review. *Annals of Botany* 125, 213–234. doi: 10.1093/AOB/MCZ161.

Lovelock, C. E., Feller, I. C., Reef, R., Hickey, S., and Ball, M. C. (2017). Mangrove dieback during fluctuating sea levels. *Scientific Reports 2017 7:1* 7, 1–8. doi: 10.1038/S41598-017-01927-6.

Mackenzie, J. R., Duke, N. C., and Wood, A. L. (2016). The Shoreline Video Assessment Method (S-VAM): Using dynamic hyperlapse image acquisition to evaluate shoreline mangrove forest structure, values, degradation and threats. *Marine Pollution Bulletin* 109, 751–763. doi: 10.1016/J.MARPOLBUL.2016.05.069.

Miles, E. R., Spillman, C. M., Church, J. A., and McIntosh, P. C. (2014). Seasonal prediction of global sea level anomalies using an ocean–atmosphere dynamical model. *Climate Dynamics* 43, 2131–2145. doi: 10.1007/S00382-013-2039-7/FIGURES/7.

Piecuch, C. G., and Quinn, K. J. (2016). El Niño, La Niña, and the global sea level budget. *Ocean Science* 12, 1165–1177. doi: 10.5194/OS-12-1165-2016.

Reef, R., and Lovelock, C. E. (2015). Regulation of water balance in mangroves. *Annals of Botany* 115, 385–395. doi: 10.1093/AOB/MCU174.

Saintilan, N., Rogers, K., and McKee, K. L. (2019). The Shifting Saltmarsh-Mangrove Ecotone in Australasia and the Americas. *Coastal Wetlands: An Integrated Ecosystem Approach*, 915–945. doi: 10.1016/B978-0-444-63893-9.00026-5.

Santini, N. S., Reef, R., Lockington, D. A., and Lovelock, C. E. (2015). The use of fresh and saline water sources by the mangrove Avicennia marina. *Hydrobiologia* 745, 59–68. doi: 10.1007/S10750-014-2091-2/FIGURES/5.

Solomon, S., Manning, M., Marquis, M., and Qin, D. (2007). *Climate change 2007-the physical science basis: Working group I contribution to the fourth assessment report of the IPCC*. Cambridge university press.

TSRA (2021). Torres Strait 2021 State of Environment Report Card. Thursday Island, Australia.

Ward, R. D., Friess, D. A., Day, R. H., and Mackenzie, R. A. (2017). Impacts of climate change on mangrove ecosystems: a region by region overview. *http://dx.doi.org.elibrary.jcu.edu.au/10.1002/ehs2.1211* 2, 1211. doi: 10.1002/EHS2.1211.

Yanoviak, S. P., Gora, E. M., Bitzer, P. M., Burchfield, J. C., Muller-Landau, H. C., Detto, M., et al. (2020). Lightning is a major cause of large tree mortality in a lowland neotropical forest. *New Phytologist* 225, 1936–1944. doi: 10.1111/NPH.16260.

Appendix A: Study sites

Table A1. The sites and coordinates (WGS84) scoped for long-term patterns in NDVI across the Torres Straits

Site	Location	Latitude S	Longitude E
TS_1	Boigu	-9.25254	142.2714
TS_2	Boigu	-9.25149	142.2718
TS_3	Boigu	-9.25699	142.2831
TS_4	Boigu	-9.25582	142.2835
TS_5	Boigu	-9.23209	142.2123
TS_6	Boigu	-9.23477	142.1384
TS_7	Boigu	-9.23678	142.1531
TS_8	Boigu	-9.23338	142.1574
TS_9	Boigu	-9.23226	142.159
TS_10	Boigu	-9.23568	142.157
TS_11	Boigu	-9.24636	142.1562
TS_12	Boigu	-9.24555	142.1588
TS_13	Boigu	-9.23844	142.1766
TS_14	Boigu	-9.24293	142.1851
TS_15	Boigu	-9.24956	142.1784
TS_16	Boigu	-9.26301	142.1321
TS_17	Boigu	-9.26724	142.1315
TS_18	Boigu	-9.27646	142.1868
TS_19	Boigu	-9.27831	142.1849
TS_20	Boigu	-9.2885	142.2428
TS_21	Boigu	-9.27784	142.2829
TS_22	Boigu	-9.24236	142.2083
TS_23	Boigu	-9.24014	142.2084
TS_24	Boigu	-9.2644	142.2574
TS_25	Boigu	-9.76868	142.6492
TS_26	Boigu	-9.24097	142.1958
TS_27	Boigu	-9.23926	142.1943
TS_28	Boigu	-9.23926	142.184
TS_29	Boigu	-9.25634	142.185
TS_30	Boigu	-9.24068	142.1608
TS_31	Boigu	-9.24662	142.1765
TS_32	Boigu	-9.23972	142.2105
TS_33	Turnagain	-9.55741	142.3012
TS_34	Turnagain	-9.55583	142.3019
TS_35	Turnagain	-9.55494	142.2927
TS_36	Turnagain	-9.55314	142.2936
TS_37	Badu	-10.073	142.14
TS_38	Badu	-10.072	142.1393
TS_39	Badu	-10.076	142.1293
TS_40	Badu	-10.0742	142.1296
TS_41	Badu	-10.0655	142.1721

TS_42	Badu	-10.0717	142.1467
TS_43	Badu	-10.0853	142.1124
TS_44	Badu	-10.1399	142.1873
TS_45	Badu	-10.1176	142.1906
TS_46	Badu	-10.1589	142.2129
TS_47	Badu	-10.1754	142.206
TS_48	Badu	-10.2139	142.2
TS_49	Badu	-10.2164	142.2077
TS_50	Moa	-10.1262	142.2585
TS_51	Moa	-10.1208	142.2653
TS_52	Moa	-10.2486	142.2714
TS_53	Moa	-10.2479	142.2669
TS_54	Moa	-10.2306	142.2283
TS_55	Moa	-10.2354	142.2593
TS_56	Moa	-10.2348	142.259
TS_57	Moa	-10.2473	142.2853
TS_58	Moa	-10.2449	142.2885
TS_59	Moa	-10.2436	142.2902
TS_60	Moa	-10.2213	142.3092
TS_61	Moa	-10.1654	142.3319
TS_62	Moa	-10.1579	142.3312
TS_63	Moa	-10.1282	142.2976
TS_64	Moa	-10.1289	142.2972
TS_65	Moa	-10.1293	142.2966
TS_66	Moa	-10.1293	142.2943
TS_67	Moa	-10.1292	142.2954
TS_68	Moa	-10.129	142.2962
TS_69	Moa	-10.1276	142.2859
TS_70	Moa	-10.1285	142.2782
TS_71	Moa	-10.1284	142.2783
TS_72	Moa	-10.1285	142.2785
TS_73	Moa	-10.1171	142.2662
TS_74	Moa	-10.1211	142.2649
TS_75	Moa	-10.1233	142.266
TS_76	Moa	-10.1294	142.2622
TS_77	Moa	-10.1322	142.2595
TS_78	Moa	-10.1239	142.2536
TS_79	POW	-10.7224	142.2096
TS_80	POW	-10.7245	142.2106
TS_81	POW	-10.7275	142.2011
TS_82	POW	-10.7292	142.205
TS_83	POW	-10.688	142.111
TS_84	POW	-10.6883	142.1102
TS_85	POW	-10.6946	142.1208

TS_86	POW	-10.6944	142.1128
TS_87	POW	-10.6966	142.1128
TS_88	POW	-10.7207	142.1193
TS_89	POW	-10.7202	142.1195
TS_90	POW	-10.7101	142.2202
TS_91	POW	-10.7165	142.2498
TS_92	Horn	-10.6215	142.249
TS_93	Horn	-10.6217	142.2479
TS_94	Horn	-10.5784	142.2768
TS_95	Horn	-10.5778	142.262
TS_96	Horn	-10.6149	142.3228
TS_97	Horn	-10.5831	142.3104
TS_98	Horn	-10.5824	142. 309595
TS_99	Horn	-10.5816	142.3096
TS_100	Horn	-10.5735	142.3001
TS_101	Horn	-10.5822	142.2751
TS_102	Horn	-10.5778	142.2616
TS_103	Horn	-10.5955	142.2439
TS_104	Horn	-10.608	142.2457
TS_105	Horn	-10.6073	142.2485
TS_106	Horn	-10.6034	142.2458
TS_107	Horn	-10.6059	142.2417
TS_108	Horn	-10.6126	142.2401
TS_109	Horn	-10.6168	142.2448
TS_110	Horn	-10.6327	142.2574
TS_111	Horn	-10.6352	142.2609
TS_112	Horn	-10.6403	142.2641
TS_113	Horn	-10.637	142.2841
TS_114	Horn	-10.5816	142.3096
TS_115	Dauan	-9.41139	142.5322
TS_116	Dauan	-9.41448	142.5283
TS_117	Erub	-9.5746	143.7789
TS_118	Erub	-9.57301	143.7793
TS_119	Erub	-9.57455	143.7798
TS_120	Erub	-9.57408	143.7801
TS_121	Erub	-9.5761	143.7833
TS_122	Erub	-9.57446	143.7796
TS_123	Erub	-9.57144	143.7768
TS_124	Saibai	-9.37307	142.7909
TS_125	Saibai	-9.37149	142.7908
TS_126	Saibai	-9.37332	142.7699
TS_127	Saibai	-9.36991	142.7697
TS_128	Saibai	-9.37391	142.6276
TS_129	Saibai	-9.37342	142.628

TS_130	Saibai	-9.37328	142.6283
TS_131	Saibai	-9.37438	142.6263
TS_132	Saibai	-9.38724	142.6074
TS_133	Saibai	-9.38436	142.6037
TS_134	Saibai	-9.39103	142.6077
TS_135	Saibai	-9.41179	142.615
TS_136	Saibai	-9.41222	142.6189
TS_137	Saibai	-9.41412	142.6208
TS_138	Saibai	-9.41927	142.6211
TS_139	Saibai	-9.42447	142.6543
TS_140	Saibai	-9.41706	142.654
TS_141	Saibai	-9.41853	142.6471
TS_142	Saibai	-9.42409	142.7168
TS_143	Saibai	-9.42495	142.7186
TS_144	Saibai	-9.42041	142.7243
TS_145	Saibai	-9.41994	142.7252
TS_146	Saibai	-9.37374	142.7915
TS_147	Saibai	-9.37238	142.7703
TS_148	Saibai	-9.36899	142.7553
TS_149	Saibai	-9.36969	142.756
TS_150	Saibai	-9.37	142.7408
TS_151	Saibai	-9.3717	142.7332
TS_152	Saibai	-9.36328	142.6655
TS_153	Saibai	-9.36902	142.6309
TS_154	Saibai	-9.38998	142.681
TS_155	Saibai	-9.40253	142.5987
TS_156	Saibai	-9.403	142.5971
TS_157	Saibai	-9.41615	142.617
TS_158	Saibai	-9.41555	142.616
TS_159	Saibai	-9.3843	142.6149
TS_160	Saibai	-9.42005	142.6257
TS_161	Gabba	-9.76956	142.642
TS_162	Gabba	-9.77307	142.6407
TS_163	Gabba	-9.77086	142.6419
TS_164	Gabba	-9.77067	142.6495
TS_165	Gabba	-9.76905	142.6469
TS_166	Gabba	-9.76662	142.6482
TS_167	Gabba	-9.76798	142.6485
TS_168	Gabba	-9.76735	142.6496
TS_169	Gabba	-9.76821	142.6498
TS_170	Gabba	-9.76868	142.6492
TS_171	Iama	-9.90111	142.7805
TS_172	Iama	-9.90156	142.7787
TS_173	Iama	-9.89822	142.78

TS_174	Iama	-9.8964	142.7762
TS_175	Iama	-9.86053	142.932442
TS_176	Iama	-9 54.078	142 46.685
TS_177	Iama	-9 54.081	142 46.290
TS_178	Iama	-9 54.083	142 46.702
TS_179	Iama	-9 54.088	142 46.708
TS_180	Iama	-9 54.183	142 46.775
TS_181	Iama	-9.90309	142.7798
TS_182	Sassie	-10.0259	142.8548
TS_183	Sassie	-10.0193	142.8464
TS_184	Sassie	-10.0343	142.8427
TS_185	Sassie	-10.0198	142.8333
TS_186	Sassie	-10.026	142.8547
TS_187	Sassie	-10.0245	142.8553
TS_188	Sassie	-10.0242	142.8547
TS_189	Sassie	-10.0239	142.8545
TS_190	Sassie	-10.0291	142.8636
TS_191	Sassie	-10.0212	142.8446
TS_192	Sassie	-10.0203	142.8343
TS_193	Sassie	-10.021	142.8329
TS_194	Sassie	-10.0221	142.8317
TS_195	Sassie	-10.0237	142.8318
TS_196	Sassie	-10.0485	142.854
TS_197	Zagai	-9.85435	142.9311
TS_198	Zagai	-9.8504	142.9328
TS_199	Zagai	-9.84819	142.9155
TS_200	Zagai	-9.84492	142.9148
TS_201	Zagai	-9.8435	142.916
TS_202	Zagai	-9.84481	142.9162
TS_203	Zagai	-9.85352	142.9447
TS_204	Zagai	-9.86053	142.9324
TS_205	Zagai	-9.86053	142.9324
TS_206	LittleAdolphus	-10.5974	142.618
TS_207	LittleAdolphus	-10.5992	142.6195
TS_208	LittleAdolphus	-10.5965	142.6211
TS_209	LittleAdolphus	-10.5993	142.6201
TS_210	LittleAdolphus	-10.5964	142.6212
TS_211	LittleAdolphus	-10.5995	142.6249
TS_212	Mori	-10.631	142.6497
TS_213	Mori	-10.6333	142.648
TS_214	Mori	-10.6515	142.6492
TS_215	Mori	-10.6504	142.6467
TS_216	Mori	-10.6299	142.6454
TS_217	Mori	-10.6292	142.645

East Cape York
Tidal Wetland Surveys 2017

Catchment Size: 104,698 ha
Tidal Wetland Area: 1549 ha
Mangrove: 1544 ha
*Saltmarsh: 5 ha**
Wetland Cover Index: 1*
River Length: 130 km
Estuary Length: 18.1 km
Estuary Size: 280 ha
Annual Rainfall: 1783 mm
Catchment Landuse
Managed Resource Protection, Grazing, Nature Conservation, Residential.

9. Endeavour River

15°27'39.267"S, 145°14'45.276"E

Tidal Wetland Threat Ranking: **5**
Cumulative Threat Score: **11.4**
Threat to tidal wetlands: Very High

Issue	Local Threat Score	Action Priority		Observations	Time Frame	Management Response		
		Estuary	East Cape York			Local	Regional	National
Upstream Bank Erosion	1.8	1	2	Mostly present in mid-estuary on southern bank. Likely to be exacerbated with sea level rise.	1.5	**Adopt living shoreline shoreline stabilizationand protection strategies**	Incentivise living shoreline strategies for landholders	**National Climate Change Policy**
Vehicles	1.5	2	11	**Vehicle tracks present in saltmarsh areas on south side. Many access points. Creating a coastal squeeze issue.**	3.5	**Restrict vehicle access**	**Improve enforcement of marine plant damage by vehicles.**	
Altered Hydrology	1.2	3	13	**Historical bund walls present on south side with ongoing impacts. Impact will increase with sea level rise.**	4	Investigate further restoration opportunities to restore natural tidal flows.		
Storm Damage	1.5	2	15	Crown damage and fallen trees in lower and mid estuary.	3			**National Climate Change Policy**
Mangrove Clearing/ Removal	1	4	17	Historical and recent removal evident in lower estuary. Ongoing trimming.	4		Maintain existing no-net loss policy.	

Other Observations: Pigs damaging lacustrine wetland areas. Many abandoned sunken vessels in the lower estuary.
*Little estuarine saltmarsh habitat mapped for this area, but larger areas of saltmarsh and saltpan were evident during surveys.

1. Bank Erosion

2. Vehicle Damage

3. Altered Hydrology

4. Storm Damage

5. Mangrove Removal